Studies on the effects of hair cosmetics on human hair by secondary ion mass spectrometry

Toru Kojima

Nagoya University

Nagoya, Japan

January 2015

Contents

Chapter 4

Compositional changes of human hair melanin resulting from bleach treatment investigated by nanoscale secondary ion mass spectrometry (NanoSIMS)

Chapter 5

Dyeing regions of oxidative hair dyes in human hair investigated by nanoscale secondary ion mass spectrometry (NanoSIMS)

Chapter 6

Investigation of dyeing behavior of oxidative dye in fine structures of the human hair cuticle by nanoscale secondary ion mass spectrometry (NanoSIMS)

Chapter 7

Chapter 1
General Introduction

Human head hair serves to protect the head from external shock, remove unnecessary metals from the body, and embellish a person's appearance. The shape, style, and color of hair significantly affect the impression of the appearance of a person, and they also express the personality of the person.

Various hair cosmetics are widely used by people who want their hair to be healthy and beautiful. On a daily basis, various treatments are performed on hair. Washing with shampoo is practiced to keep the hair and scalp clean. Hair conditioner is used to provide softness, smoothness, and glossiness to hair. Daily hair care routines such as brushing, drying using a hair dryer, and setting of a hairstyle using a hair iron are also performed. Hair is weathered by exposure to ultraviolet radiation from sunlight. Additionally, chemical treatments such as permanent waving, bleaching, and hair coloring can significantly change the appearance of hair. They are used by many people who wish to modify their natural style and hair color to a desired style and color.

Human hair structure

Human hair is a biological material comprising various morphological structures. The most abundant protein contained in hair is keratin, which has rich cystine content in an amino acid composition. Hair fiber has a hierarchical structure: the cuticle, cortex, and medulla (Figure 1.1) [Zvaik et al., 1986; Swift, 1997; Popescu et al., 2007; Robbins, 2012a]. The medulla, which is central axis of the hair, has a honeycomb-like structure. The cortex constitutes the majority of the hair structure and comprises macrofibril, intermacrofibrillar matrix, nuclear remnant, and melanin pigment. The spindle-shaped cortical cells are approximately 1–6 μm in diameter and 100 μm in length. The macrofibril is a major component of the cortical cells and has a diameter of approximately 100–400 nm. Each macrofibril comprises microfibril (intermediate filament (IF)), which is a low-sulfur-content protein, and the matrix, which is a high-sulfur-content and globular protein. Melanin pigments are ellipsoidal granules that approximately 0.4–1.2 μm in length and 100–500 nm in diameter [Wolfram et al., 1970;

Zvaik et al., 1986; Arnaud et al., 1981; Robbins, 2012c], and they are biosynthesized from the amino acid tyrosine, catalyzed by tyrosinase in the melanocytes (Figure 1.2) [Prota, 1988; Ito et al., 2000]. Although the content of melanin granules in human hair is a few weight percent [Menkart et al., 1966; Arnaud et al., 1981], these granules determine the natural hair color. The cuticle surrounding the cortex generally consists of 5–10 overlapping layers. The thickness of each cuticle cell is approximately 500 nm. The cuticle comprises three major layers that have different cystine contents in the amino acid composition. These layers are the A-layer, exocuticle, and endocuticle (Figure 1.3) [Hallegot et al., 1993; Swift, 1999; Bhushan, 2010]. The A-layer has the highest cystine content (~30%) among the three layers of the cuticle, and its thickness is ~100 nm. The exocuticle, too, is rich in cystine (~20%). The A-layer and exocuticle are regions with high cystine content and are highly cross-linked by the disulfide bonds of cystine. The endocuticle comprises nonkeratinous protein and has low cystine content (~3%). The exocuticle and endocuticle are inhomogeneously thick layers and are approximately a few hundred nanometers thick. The cuticle layers and cortical cells are separated from each other by the cell membrane complex (CMC), which has a structure sandwiching the δ-layer, comprising protein, between the two β-layers, which are lipid layers [Naito et al., 1992; Robbins, 2012a].

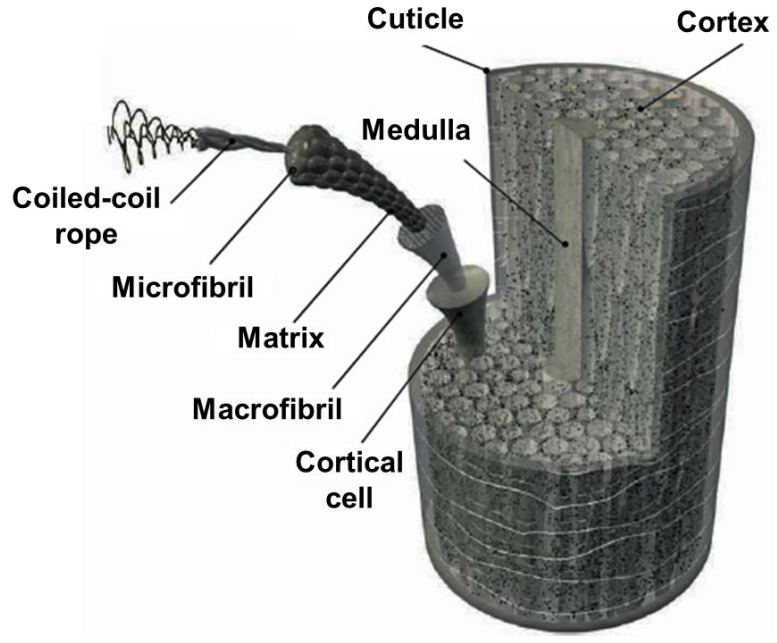

Figure 1.1 Schematic view of hierarchical structure of human hair fiber [Zvaik et al., 1986; Swift, 1997; Popescu et al., 2007; Robbins, 2012a].

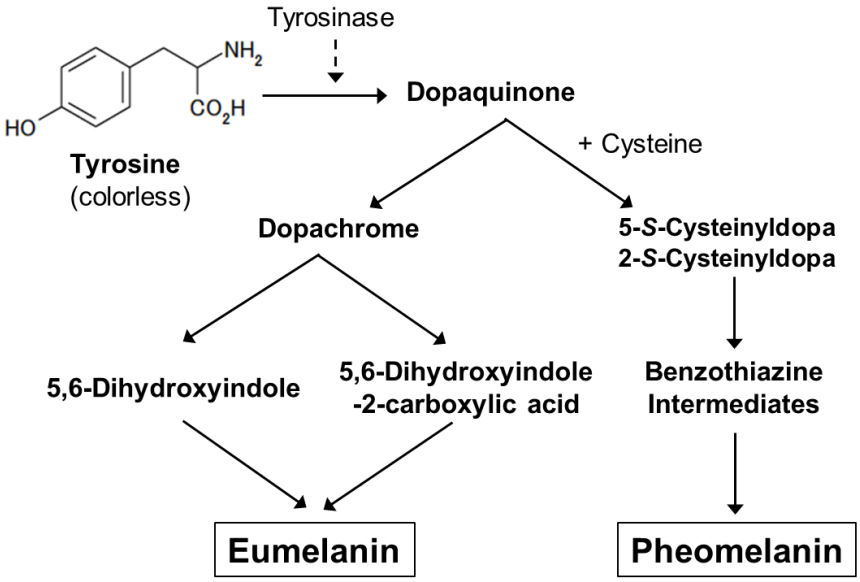

Figure 1.2 Biosynthetic pathways of melanin [Prota, 1988; Ito et al., 2000].

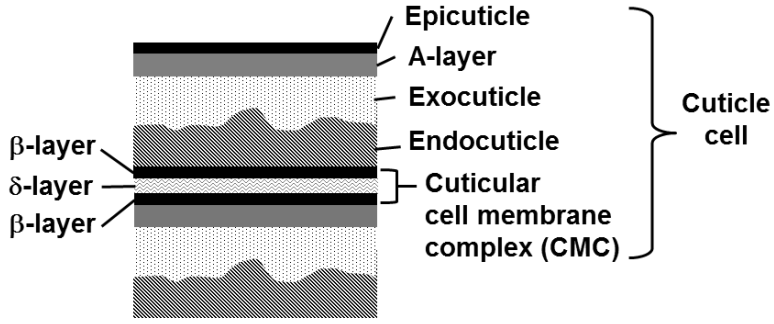

Figure 1.3 Fine structures of hair cuticle layer [Hallegot et al., 1993; Swift, 1999; Bhushan, 2010].

Chemical treatments for human hair

Permanent waving, hair coloring, and bleaching, which are widely used to change the style and natural color of hair, are typical chemical treatments for hair.

Permanent hair waving is used by those who want to permanently modify their hair to a desired shape and style. The purpose of permanent waving is to realize a wavy hairstyle [Robbins, 2012b; Wickett, 2012]. First, the hair is washed and physically rearranged from the original to the intended hairstyle by using rods or curlers. Then, a perm solution containing a reducing agent such as thioglycolic acid or L-cysteine is

applied on the hair to cleave the disulfide bonds of cystine in the hair keratin protein. In most cases, an alkaline perm solution is used in order to swell the hair and for the reducing agent to penetrate the hair. After a certain period of time, the perm solution is rinsed off from the hair with water, and then, a neutralizing solution containing an oxidative agent such as hydrogen peroxide or sodium bromate is applied on the hair to recombine the disulfide bond and to hold the waved hairstyle.

Hair coloring is one of the most important chemical treatments in hair cosmetic processes because many people worldwide widely use it to change their original hair color and/or to cover their gray hair. Various types of hair coloring products such as temporary, semi-permanent, and permanent are commercially available. Among them, permanent (oxidative) hair coloring products are particularly important. Oxidative hair colorant is a major hair coloring product because of its broad ranges of tonality and brightness. In addition, the resulting hair color from the oxidative hair coloring lasts longer than other hair coloring methods. Generally, oxidative hair coloring products come in kits; colorant containing several types of oxidative hair dyes and alkaline agents is mixed with a developer containing an oxidizing agent, typically hydrogen peroxide. The colorant and developer are mixed immediately before use, and the resulting mixture is applied to the hair for coloring. The dyeing mechanism of an oxidative hair-coloring product simultaneously bleaches melanin pigments and forms colored chromophores from the oxidative dyes in the hair fiber [Zvaik, 1986; Brown, 1997; Morel et al., 2011; Marsh, 2012; Robbins, 2012d]. Figure 1.4 shows typical oxidative dyes. The primary intermediates—*p*-phenylenediamine, *p*-aminophenol, and their derivatives—produce color, usually a dark shade, by oxidative dyeing. They also produce various color shades by reacting with couplers such as *m*-aminophenol, its derivatives, and resorcinol in oxidative dyeing. Oxidative dyes, which are initially uncolored dye precursors, penetrate the hair and are oxidized by the oxidizing agent. Consequently, colored chromophores are developed inside the hair fiber. Figure 1.5 shows typical colored chromophores formed in oxidative dyeing. Melanin pigments are also bleached by alkaline hydrogen peroxide in oxidative dyeing, as a result of which the hair color becomes brighter than the original hair color. The development of colored chromophores and decoloration of melanin during oxidative dyeing determine the final hair color after oxidative dyeing.

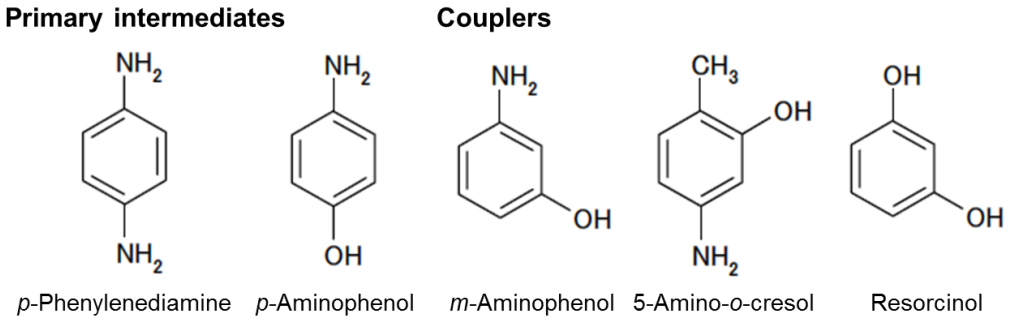

Figure 1.4 Chemical structures of typical oxidative dyes.

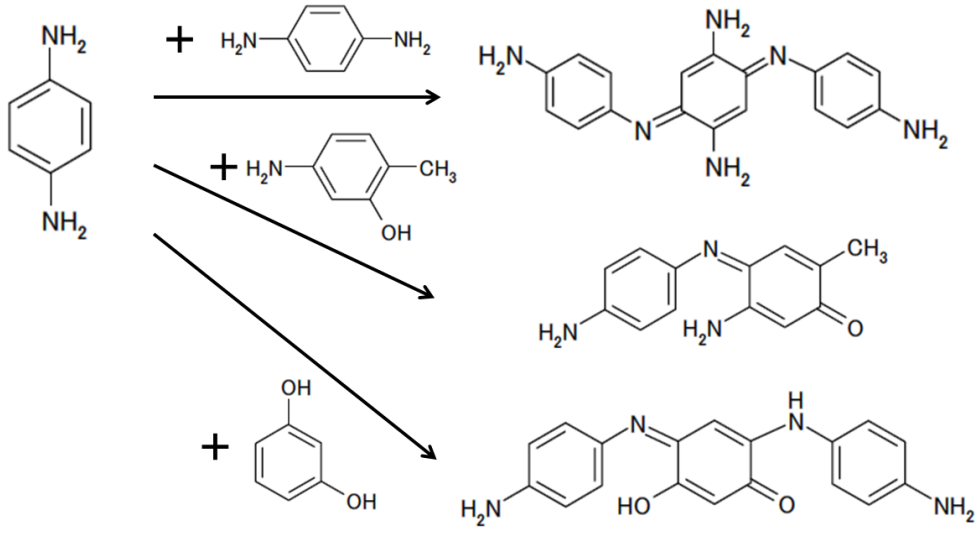

Figure 1.5 Typical colored chromophores formed in oxidative dyeing.

Bleaching products are used to lighten the original hair color by decolorizing the melanin in hair [Wolfram et al., 1970; Brown, 1997; Marsh, 2012; Robbins, 2012c]. An oxidizing agent, typically hydrogen peroxide, is mixed with alkaline agents such as ammonia and ethanolamine prior to use, and the resulting mixture is applied to hair for bleaching. If significantly bright hair color is required with a single round of bleaching, some persulfates are added as bleach boosters.

These chemical treatments also cause undesirable changes in hair, namely, hair damage.

Hair damage and hair care

Hair damage is caused by chemical treatments; by daily hair care routines such as brushing, heat drying, and setting of hairstyle using a hair iron; and by weathering, especially exposure to ultraviolet radiation from sunlight [Masukawa et al., 2004; Tanamachi et al., 2004; Popescu, 2012]. Undesirable changes are induced in the morphological, chemical, and physical properties of hair by such damage. People notice these changes from the hair texture and physical appearance of hair. Hair comprises dead cells and does not have the ability to repair itself. To remedy the hair condition and prevent further hair damage, it is important to care for and repair damaged hair using conditioning agents. Various conditioning agents, such as amino acids, vegetable oils, silicones, cationic surfactants, cationic polymers, and hydrolyzed proteins are used to improve the condition and texture of damaged hair [Hoshowski, 1997; Lochhead, 2012].

Methods for evaluating hair

Hair damage caused by various factors affects the hair characteristics. To develop hair cosmetics with better performance for damaged hair, it is important to understand the influences of damage on the hair characteristics. The changes in hair characteristics are measured by using various evaluation methods. The influence on the mechanical properties of hair has been measured using a tensile tester [Jachowicz, 1987; Tate et al., 1993], bending tester [Wortmann et al., 1990], and torsion tester [Wortmann et al., 1985]. Recently, atomic force microscopy (AFM) has been used to evaluate the mechanical properties of the hair micro region under ambient conditions, such as in air and water [Chen et al., 2005; Kitano, 2009]. The morphological changes resulting in hair from chemical treatments have been observed by scanning electron microscopy (SEM) [Tate et al., 1993; Takada et al., 2003], transmission electron microscopy (TEM) [Imai, 2011; Kuzuhara, 2013], and laser scanning microscopy (LSM) [Corcuff et al., 1993]. The compositional changes occurred in hair by damage are often evaluated by amino acid analysis [Robbins et al., 1969; Wolfram et al., 1970; Gumprecht et al., 1977; Chao et al., 1979]. Vibrational techniques such as infrared, Raman spectroscopy and

their microspectroscopies have often been used to determine the structural changes caused by chemical treatments on the surface of and inside hair [Bantignies et al., 1998 and 2000; Kuzuhara 2005, 2006, 2007, and 2013]. These techniques have revealed the cleavage of the disulfide bond in the hair cuticle and cortex regions and the formation of cysteic acid. To deepen the understanding of the hair damages, it is necessary to investigate the influences on the micro region of each hair tissues.

Methods for evaluating distributions of cosmetic ingredients in human hair

It is important to understand the functional mechanism of cosmetic ingredients such as conditioning agents and active ingredients of chemical treatments on hair. The action site of the cosmetic ingredient on hair is great importance in conjunction with the effect of the cosmetic ingredient on hair.

The repairing effect of conditioning agents on damaged hair is considered to be caused by adsorption on the hair surface and penetration into hair. However, the distribution and penetration of conditioning agents on hair have not been clarified in adequate detail. The fluorescent labeling method combined with fluorescence microscopy is frequently used to estimate the distribution of cosmetic ingredients on hair [Regismond et al., 1999; Swift et al., 2000; Gruber et al., 2001]. However, this labeling method causes structural changes in the cosmetic ingredients by introducing a fluorescence reagent and may affect the permeability and adsorptive property of the cosmetic ingredients. The dyeing method is also used to investigate the permeability of cosmetic ingredients [Kuzuhara et al., 2003; Kuzuhara, 2011]. Cosmetic ingredients having a carboxyl group in their chemical structures, such as amino acids and peptides, were negatively charged above the isoelectric point. After a cosmetic ingredient having a carboxyl group was applied on hair, a hair cross-section was prepared and then dyed with a basic dye that has a positive charge in its chemical structure. Because the cosmetic ingredient penetrating the hair was dyed by a basic dye, the permeability of its ingredient could be evaluated by optical microscopy observation of the dyed hair cross-section. However, this dyeing method can be applied to only limited cosmetic ingredients. Although these evaluation methods are useful for investigating the action sites of cosmetic ingredients, they have some drawbacks. Therefore, an evaluation

method that can more directly analyze the cosmetic ingredients on hair is desired.

Hair dye is one of the most interesting cosmetic ingredients from the viewpoint of its functional mechanism on hair. For hair dyeing, various hair dyes such as oxidative, acid, and basic dyes are used. Among these dye types, oxidative dye is particularly important because oxidative hair coloring is widely used worldwide. To develop a more effective oxidative hair coloring product and hair care product for maintaining colored hair, it is important to further understanding of the dyeing behaviors of oxidative coloring on hair. The dyeing regions of hair coloring and the dyeing degree of these regions are both of great importance. The penetration and distribution of hair dyes in the hair fiber have been investigated by observing cross-sections of dyed hair using an optical microscope, and it is confirmed that the cuticle and cortex are major dyeing regions of oxidative hair coloring [Wilmsmann, 1961; Imai et al., 2008]. However, the dyeing behavior of oxidative dye in the fine structures of hair has not yet been confirmed because these structures cannot be identified by optical microscopy and the dye location cannot be evaluated by conventional techniques for observing the hair structure, such as SEM and TEM. On the other hand, fluorescent dyes can be used to evaluate the penetration pathway and diffusion of applied cosmetic ingredients in hair and dyeing regions. The penetration and adsorption of a fluorescent dye were investigated by fluorescence microscopy [Tate et al., 1993; Regismond et al., 1999], confocal laser scanning microscopy (CLSM) [Corcuff et at al., 1993; Swift et al., 2000], and scanning near-field optical microscopy (SNOM) [Kelch et al., 2000; Formanek et al., 2006]. CLSM and SNOM with high spatial resolution showed that the fluorescent dye localized in the endocuticle and other fine structures of the hair. However, these fluorescent techniques cannot be used for evaluating the dyeing behavior of oxidative hair coloring because the chemical structure and dyeing mechanism of the fluorescent dye are quite different from those of the oxidative dye. As a result, the dyeing behaviors of oxidative dyes in fine structures of human hair have not yet been determined by conventional techniques.

Secondary ion mass spectrometry

Secondary ion mass spectrometry (SIMS) is a direct surface analysis technique that

can provide information about the elemental, isotopic, and molecular distribution on solid sample surfaces, and it has been used in various research fields such as semiconductor engineering, material sciences (e.g., metals, ceramics, and polymers), geoscience, and space science. Furthermore, SIMS has been increasingly applied to biological materials in recent years [Lechene et al., 2006; Clode et al., 2007 and 2009; Herrmann et al., 2007; Saito et al., 2008 and 2012].

Figure 1.6 shows a schematic view of the SIMS process. A focused primary ion beam is irradiated on the sample surface. By the impact of the primary ions, surface sputtering occurs and various particles such as secondary ions, neutral atoms, and molecular fragments are emitted from the sample surface. The secondary ions in these particles are measured by a mass analyzer. Atomic ions such as Ar^+, Cs^+, Ga^+, Au^+, and O^- have been used as primary ion beams. Recently, cluster ions such as Au_n^+, Bi_n^+, Ar_n^+, and C_{60}^+ have been used to obtain higher secondary ion yields, especially in the range of large molecular fragment ions. Quadrupole, time-of-flight, and magnetic sector type mass analyzers have been used. SIMS analysis is advantageous in that it can simultaneously measure the mass spectrum and the secondary ion image obtained by the scanning of the focused primary ion beam on the sample surface.

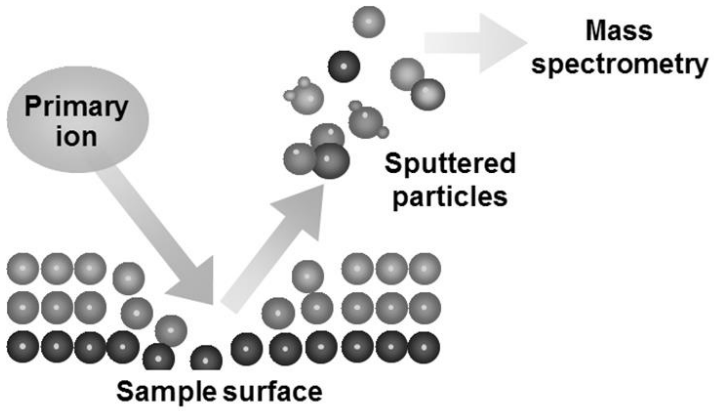

Figure 1.6 Schematic view of SIMS process.

SIMS is classified into two types by the dose amount of the primary ion during analysis: static SIMS ($\leq 1\times10^{12}$ ions/cm^2) and dynamic SIMS [Boxer et al., 2009]. In dynamic SIMS, which is a destructive analysis method, a continuous beam is irradiated on the sample surface to mainly analyze the distributions of elemental, isotopic, and

diatomic ions. Furthermore, dynamic SIMS is useful for the high-sensitivity analysis and depth profiling of trace elements by sputtering with a continuous beam. Nanoscale SIMS (NanoSIMS) is a type of dynamic SIMS that has high spatial resolution and sensitivity for imaging the distribution of secondary ions on sample surfaces [Herrmann et al., 2007; Boxer et al., 2009]. In NanoSIMS measurement, five (NanoSIMS 50) or seven (NanoSIMS 50L) kinds of ions can be detected in parallel, and it is necessary to preselect the measuring ions. In comparison with dynamic SIMS, static SIMS is a non-destructive analysis method. It irradiates a pulsed primary ion beam on the sample surface and can detect not only elemental and isotopic ions but also large fragment ions keeping the information related to the chemical structure. Additionally, static SIMS can be used to obtain the information about outermost surface of a sample, which is a few atomic layers thick. Time-of-flight SIMS (TOF-SIMS) is a type of static SIMS that can measure a wide mass range at once with high mass resolution and sensitivity.

SIMS is also used in combination with the isotope labeling technique. The isotope labeling of a compound of interest does not cause major changes in its chemical characteristics, and the isotope becomes a high-selectivity tracer for analyzing the behavior of the target compound in tissue. Therefore, SIMS can be used to investigate the distribution and localization of an isotope-labeled compound within biological materials [Lechene et al., 2006; McMahon et al., 2006; Clode et al., 2007 and 2009].

In hair research, SIMS has been used to investigate the adsorptive properties, permeabilities, and localizations of cosmetic ingredients [Berthiaume et al., 1995; Ruetsch et al., 2001 and 2005; Harvey et al., 2004; Staudigel et al., 2007] and trace metals [Audinot et al., 2004; Kempson et al., 2005; Smart et al., 2009] in hair. However, SIMS still finds limited applications in hair research. Widening the use of SIMS in hair research is expected to provide better understandings of the functional mechanisms of cosmetic ingredients on hair fibers and the influences of chemical treatments on hair tissue.

Outline of this thesis

This thesis is entitled “Studies on the effects of hair cosmetics on human hair by secondary ion mass spectrometry”, and it consists of seven chapters. This study aims to

use SIMS to obtain better understandings of the functional mechanisms of hair cosmetics on human hair by investigating the location of cosmetic ingredients and evaluating the compositional changes in hair tissue. In this thesis, two types of SIMS, TOF-SIMS and NanoSIMS, were used, and the advantages of each analysis technique were exploited. Figure 1.7 shows photographs of the two types of SIMS used in this thesis.

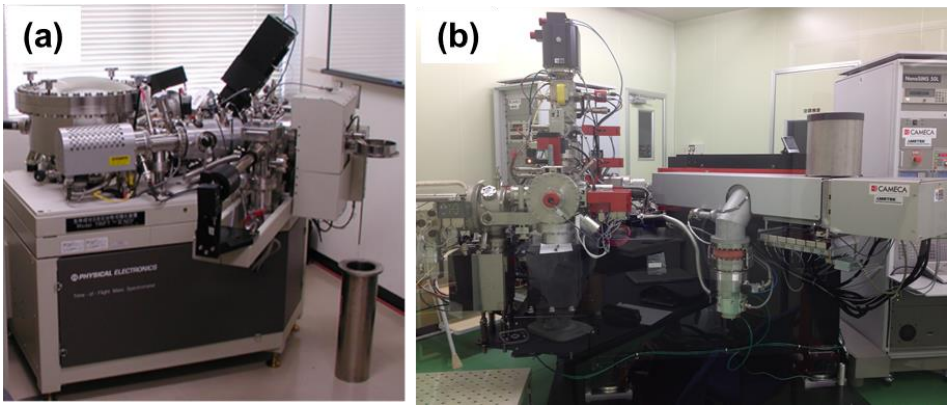

Figure 1.7 Photographs of two types of SIMS: (a) TOF-SIMS (TRIFT III spectrometer, ULVAC-PHI, Japan), (b) NanoSIMS (NanoSIMS 50, Cameca, France).

Chapter 2 describes the investigation of the penetration and adsorption of two cosmetic ingredients on hair by TOF-SIMS.

Chapter 3 describes the evaluation of the conditioning effect of vegetable oil for damaged hair and the investigation of the permeability of this vegetable oil by TOF-SIMS.

Chapter 4 describes the influence of bleach treatment on the chemical composition of human hair melanin by the investigation of NanoSIMS.

Chapters 5 and 6 describe the investigation of the dyeing regions of oxidative hair dyes in the fine structure of human hair by using a stable isotope-labeled oxidative dye with NanoSIMS. In particular, Chapter 6 focuses on the dyeing behavior in the fine structures of the hair cuticle.

Chapter 7 summarizes the results obtained in this thesis.

Chapter 2
Imaging analysis of cosmetic ingredients interacted with human hair using time-of-flight secondary ion mass spectrometry (TOF-SIMS)

2.1. Introduction

Hair damage is caused by various factors such as chemical treatments, hair care routines, and weathering. Various cosmetic ingredients have been developed to repair hair damage. It is important to know the distribution of cosmetic ingredients on damaged hair to understand their interaction mechanisms with hair. A previous study reported that L-theanine restored the mechanical properties of damaged hair [Kitano, 2008]. Because the mechanical property of hair is mainly related to the hair cortex, the penetration of L-theanine was investigated. On the other hand, cationic chitosan is used as the conditioning agent to improve the texture of the hair surface. Therefore, the adsorption of cationic chitosan was investigated. In this chapter, the distribution of two cosmetic ingredients, L-theanine and cationic chitosan, on hair was investigated by TOF-SIMS.

2.2. Materials and Methods

Materials

Japanese hairs which had never been chemically treated, taken approximately 5 cm from the root, were used.

25 wt% ammonia solution (Wako Pure Chemical Industries, Japan), 30 wt% hydrogen peroxide (Wako Pure Chemical Industries, Japan), thioglycolic acid (Wako Pure Chemical Industries, Japan), 2-aminoethanol (Wako Pure Chemical Industries, Japan), sodium bromate (Wako Pure Chemical Industries, Japan), L-theanine (Taiyo Kagaku CO., LTD., Japan), deuterium-labeled L-theanine (ethyl-d_5) (Taiyo Kagaku CO., LTD., Japan), and cationic chitosan aqueous solution (Katakura Chikkarin Co., Ltd.,

Japan) were used without further purification.

Damage treatments for the hair

Damaged hairs were chemically treated by performing bleaching and permanent waving. Bleaching was performed for 30 min at 30°C in an aqueous solution containing 1 wt% ammonia and 3 wt% hydrogen peroxide. Permanent waving was performed for 10 min at 30°C using an aqueous solution containing 6 wt% thioglycolic acid at pH 9 adjusted by 2-aminoethanol. After rinsing with purified water, the waved hair was oxidized for 10 min at 30°C using 6 wt% sodium bromate aqueous solution.

Hair treatment using L-theanine

The damaged hair, which was bleached twice and was performed permanent waving once, was immersed in 5 wt% L-theanine or deuterium-labeled L-theanine aqueous solution for 10 min at 30°C. Then, this hair was briefly rinsed with purified water and dried with a hair dryer. The hair was cross-sectioned using an uncoated steel blade.

Hair treatment using cationic chitosan

Hair that has not been chemically treated is called virgin hair. Virgin hair and damaged hair that was bleached once were immersed in 0.1 wt% cationic chitosan aqueous solution for 5 min at 30°C. Then, these hairs were rinsed in purified water for 60 s and dried with the hair dryer.

TOF-SIMS measurements

TOF-SIMS measurements were performed using a TRIFT III spectrometer (ULVAC-PHI, Japan). Positive and negative ion spectra were obtained using a 22 keV Au_1^+ primary ion beam operated at a current of 0.7 nA, with a pulse width of 10 ns. The primary ion beam was rastered over a surface area of 125 × 125 μm for visualizing the

distribution of L-theanine, and over a surface area of 200 × 200 μm for visualizing the distribution of cationic chitosan. A low-energy pulsed electron gun (28.0 eV) was used for surface charge compensation.

SEM measurement

The hair surface was observed by SEM. The hair was coated with a layer of platinum, and then measured using a JEOL JSM-5600LV scanning electron microscope (JEOL, Japan).

2.3. Results and Discussion

Penetration of L-theanine into the hair

I examined the cross-section of the hair treated using L-theanine. However, it was difficult to detect the molecular and fragment ion peaks derived from L-theanine in the positive and negative TOF-SIMS spectra of the hair. Therefore, L-theanine was deuterium-labeled to detect the deuterium ion at *m/z* 2 as a characteristic fragment ion peak of L-theanine. Figure 2.1 shows the negative TOF-SIMS spectra of L-theanine and deuterium-labeled L-theanine (ethyl-d_5). The spectrum of deuterium-labeled L-theanine clearly showed peaks of the deuterium ion at *m/z* 2 and the molecular ion of deuterium-labeled L-theanine at *m/z* 178 (Figure 2.1(b)). Further, the negative TOF-SIMS spectrum of the damaged hair treated using deuterium-labeled L-theanine in comparison with untreated clearly showed the deuterium ion peak (Figure 2.2(a)). Furthermore, deuterium ion mapping was carried out to estimate the degree of penetration of L-theanine (Figure 2.3). The mapping image of the deuterium ion revealed that L-theanine penetrated deep and was distributed uniformly inside the damaged hair.

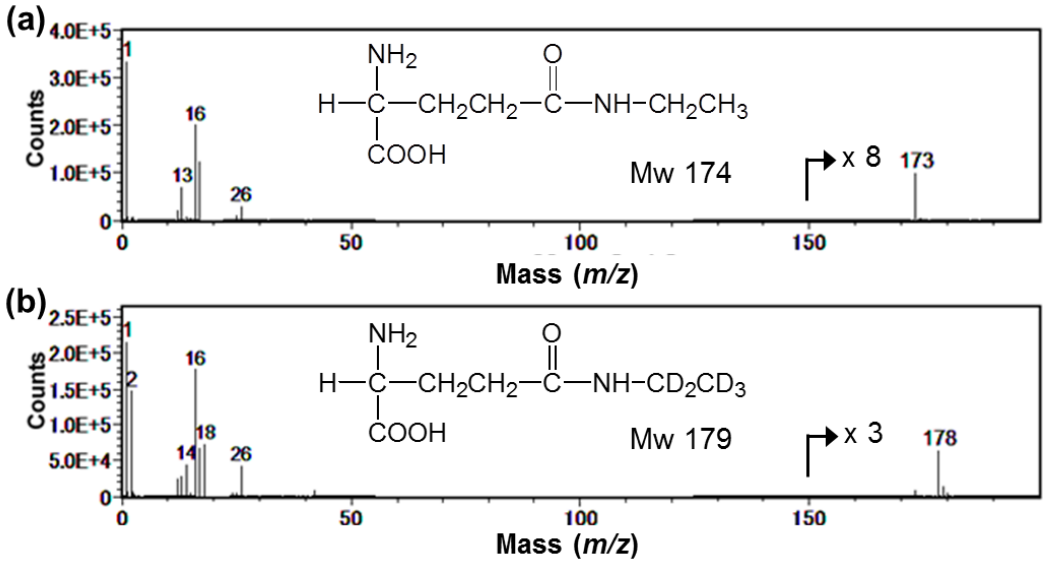

Figure 2.1 Negative TOF-SIMS spectra (*m/z* = 0–200): (a) L-theanie, and (b) deuterium-labeled L-theanine (ethyl-d_5).

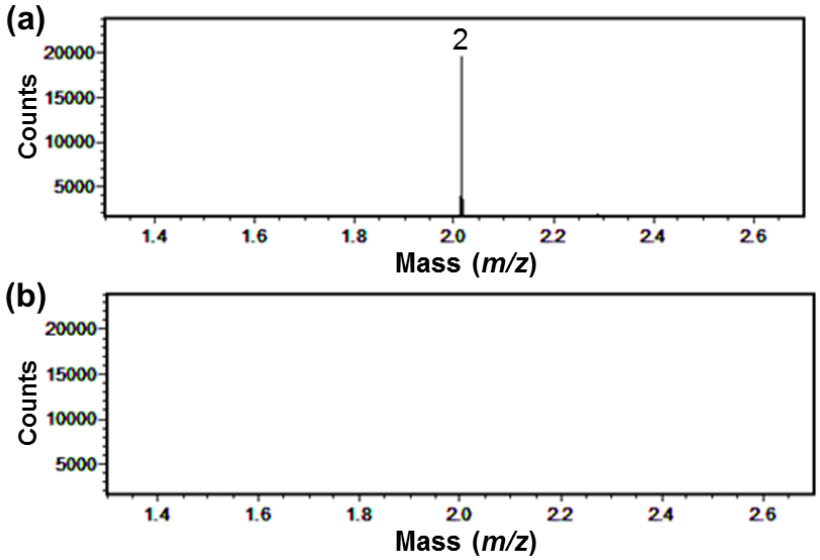

Figure 2.2 Negative TOF-SIMS spectra of the damaged hair cross-section (*m/z* = 1.3–2.7): (a) treated using deuterium-labeled L-theanine, and (b) untreated.

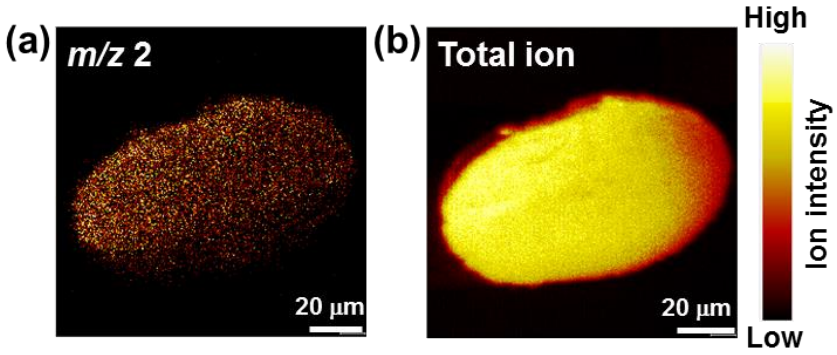

Figure 2.3 TOF-SIMS negative ion images of the damaged hair cross-section treated using deuterium-labeled L-theanine: (a) deuterium ion (*m/z* 2) image, and (b) total ion image.

Adsorption of cationic chitosan on hair surface

Figure 2.4(a) shows the positive TOF-SIMS spectra of cationic chitosan. The most intensive peak at *m/z* 58 was not suitable for hair surface analysis, because this peak was detected from the hair surface untreated using cationic chitosan (Figure 2.4(b)). Therefore, I focused on the fragment ion peak at *m/z* 102. The ion peak at *m/z* 102 was identified as $C_5H_{12}NO^+$ ion (exact mass = 102.0918). A previous study carried out using cationic starch, which has the same cationic group as cationic chitosan, indicated that the ion peak at *m/z* 102 was a fragment ion having the cationic trimethylammonium group [Matsushita et al., 2007].

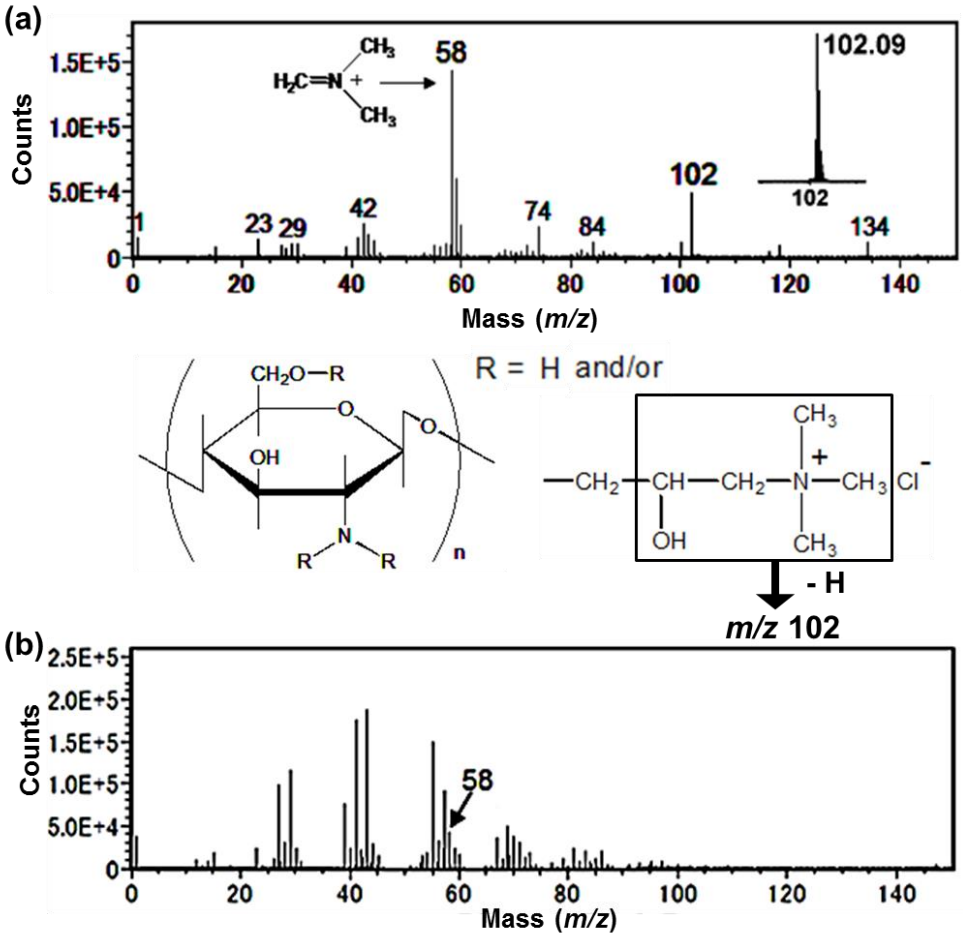

Figure 2.4 Positive TOF-SIMS spectra (*m/z* = 0–150): (a) cationic chitosan. The structure of secondary ion at *m/z* 102 is shown: $C_5H_{12}NO^+$ (exact mass = 102.0918), and (b) hair surface untreated using cationic chitosan.

Figure 2.5 shows the positive TOF-SIMS spectra of the hair surface treated using cationic chitosan. The peak at *m/z* 102 was detected from the hair surface. This peak was more clearly visible in the spectrum of the bleached hair than in the spectrum of the virgin hair (Figure 2.5). Figure 2.6 shows TOF-SIMS positive ion images and an SEM image of the hair surface treated using cationic chitosan. The mapping image of *m/z* 102 ion revealed that cationic chitosan was uniformly adsorbed on the hair surface. The difference in the amount of adsorbed cationic chitosan between the virgin and bleached hair was visualized. It is known that the outermost surface of human hair is coated with a lipid monolayer called epicuticle, which is mainly composed of 18-methyleicosanoic acid (18-MEA) bounded to the protein via a thioester linkage [Negri et al., 1993; Jones

et al., 1997; Swift, 1999]. The epicuticle is damaged by bleaching, which causes the cleavage of the thioester linkage and the formation of cysteic acid group (Figure2.7) [Robbins et al., 1984; Strassburger et al., 1985; Nishida et al., 2004; Masukawa et al., 2004, Beard et al., 2005; Okamoto et al., 2011; Habe et al., 2011]. The formation of cysteic acid group by bleaching leads to an increase in the negative charge on the hair surface. The results of Figure 2.5–2.7 indicated that the amount of cationic chitosan adsorbed on the bleached hair was more than that on the virgin hair, because bleaching resulted in an increase of negative charge derived from the formation of cysteic acid group.

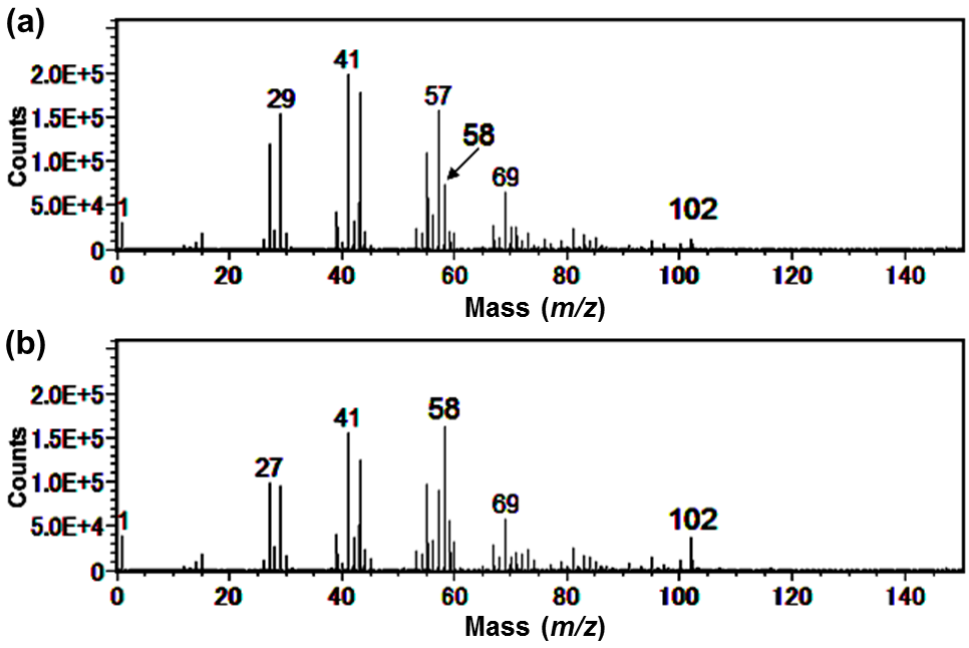

Figure 2.5 Positive TOF-SIMS spectra of the hair surface treated using cationic chitosan (*m/z* = 0–150), (a) virgin hair, and (b) bleached hair.

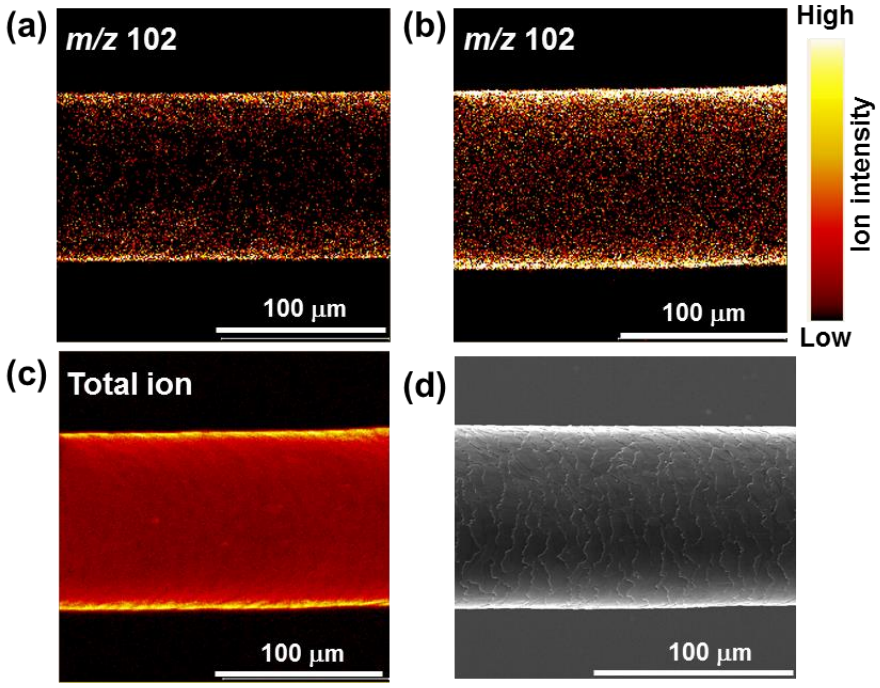

Figure 2.6 TOF-SIMS positive ion images and SEM image of the hair surface treated using cationic chitosan: (a)–(c) TOF-SIMS ion images; (a) virgin hair (*m/z* 102), (b) bleached hair (*m/z* 102), (c) bleached hair (total ion), and (d) SEM image of bleached hair.

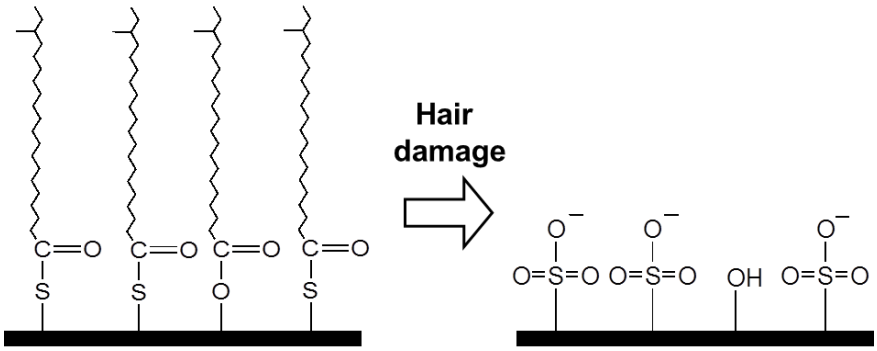

Figure 2.7 Schematic view of hair surface.

2.4. Summary

The penetration and adsorption of two cosmetic ingredients on human hair were investigated by TOF-SIMS. The TOF-SIMS imaging analysis revealed that L-theanine

penetrated deeply and was distributed uniformly over the damaged hair inside. Further, TOF-SIMS ion images revealed that cationic chitosan was uniformly adsorbed on the hair surface. The difference in the amount of adsorbed cationic chitosan between virgin and bleached hair was visualized.

Chapter 3
Distribution analysis of triglyceride having repair effect on damaged human hair by time-of-flight secondary ion mass spectrometry (TOF-SIMS)

3.1. Introduction

Undesirable changes are induced in the morphological, chemical, and physical properties of hair by hair damage. One of the undesirable changes caused by hair damage is an increase in the degree of swelling of hair in water (Figure 3.1). A swelling test is used to evaluate hair damage because the degree of hair swelling is dependent on the degree of hair damage [Klemm et al., 1965]. Damaged hair with a high degree of swelling is susceptible to further damage by weathering and daily hair care practices such as brushing and blow drying. Hair comprises dead cells and does not have the ability to repair itself. Therefore, it is important to repair damaged hair using conditioning agents to prevent further hair damage. Vegetable oils are widely used as conditioning agents in hair care products. It was reported that some vegetable oils have beneficial effects on hair [Rele et al., 2003; Keis et al., 2005 and 2007]. In this chapter, an effective vegetable oil for inhibiting the swelling of damaged hair was focused on. It is considered that the repairing effect of a conditioning agent on damaged hair is caused by adsorption on the hair surface and penetration into the hair. To understand the functional mechanism of vegetable oil in the inhibition of the swelling of damaged hair, the penetration of oil into damaged hair was investigated by TOF-SIMS.

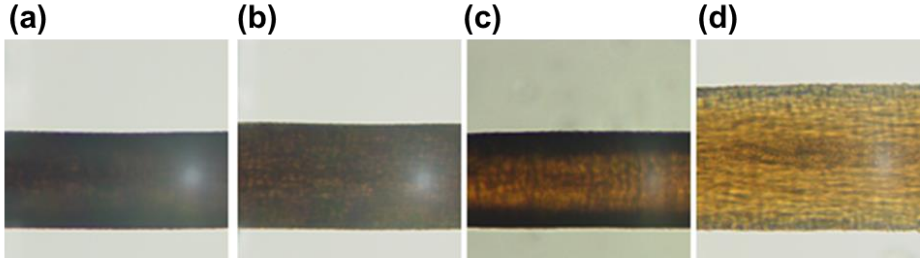

Figure 3.1 Optical microscope images of hair swelling behavior in water: (a) and (b) healthy (undamaged) hair; (a) dry, (b) water-swollen, and (c) and (d) chemically damaged hair; (c) dry, (d) water-swollen.

3.2. Materials and Methods

Materials

I used chemically undamaged black human hair.

25wt% ammonia solution (Wako Pure Chemical Industries, Japan), 30wt% hydrogen peroxide (Wako Pure Chemical Industries, Japan), thioglycolic acid (Wako Pure Chemical Industries, Japan), 2-aminoethanol (Wako Pure Chemical Industries, Japan) and sodium bromate (Wako Pure Chemical Industries, Japan) were used without further purification.

Hydrogenated palm oil (Nikko Chemicals, Japan), which characteristically has much saturated fatty acids in the molecular structure of its triglycerides, was used. Tripalmitin (Tokyo Chemical Industry, Japan) and deuterium-labeled tripalmitin, tripalmitin-d_{98}, (C/D/N Isotopes Inc., Canada), were used as indicators of hydrogenated palm oil. Cetostearyl alcohol (New Japan Chemical Co., Ltd., Japan), which is a pre-mixture of 1-hexadecanol and 1-octadecanol, and cationic surfactant (Evonik Japan, Japan), which is a pre-mixture of behenyl trimethyl ammonium chloride and isopropyl alcohol , were used to prepare the hair conditioners containing the vegetable oil.

Damage treatments for hair

The damaged hair sample was prepared by bleaching and permanent waving treatments, carried out twice alternately. Bleaching was performed for 30 min at 30°C in an aqueous solution containing 1wt% ammonia and 3wt% hydrogen peroxide. Permanent waving was performed for 10 min at 30°C by using an aqueous solution containing 6wt% thioglycolic acid at pH 9 adjusted with 2-aminoethanol. After rinsing with water, the waved hair was oxidized for 10 min at 30°C by using an aqueous solution containing 6wt% sodium bromate.

Treatment with conditioner

The damaged hair samples were treated with each hair conditioner, shown in Table

3-1, for 30 min at 40°C. The samples were then briefly rinsed with water and dried with a hair dryer.

Table 3.1 Formulation of hair conditioners (w/w %)

	Control	With hydrogenated palm oil
Cetostearyl alcohol	5.0	5.0
Cationic surfactant	2.5	2.5
Hydrogenated palm oil	-	5.0
Water	to 100	to 100

Hair swelling test

The hair samples were immersed in water for 10 min. The radius (r) of the samples was measured using an optical microscope before and after conditioning treatment. Assuming that the cross-sectional shape of the hair was a true circle, the degree of hair swelling after conditioning was calculated from the equation (1):

$$\text{Degree of swelling (\%)} = 100 \times (r_1^2 (r_4^2 - r_3^2)) / (r_3^2 (r_2^2 - r_1^2)) \qquad (1)$$

where r_1 (dry) and r_2 (water-swollen) are the radii of the hair before conditioning treatment, and r_3 (dry) and r_4 (water-swollen) are the radii after conditioning treatment.

Gas chromatographic (GC) analysis

GC analysis with a flame ionization detector was performed using an Agilent 6890 GC Series (Agilent Technologies Inc, California) equipped with a DB-5HT column (30 m × 0.25 mm ID and 0.1 μm film thickness) (Agilent Technologies Inc, California). An initial column temperature of 300°C was maintained for 2 min and then increased to 400°C at a rate of 20°C/min.

LSM measurement

LSM was performed using a VK-8710 laser scanning microscope (KEYENCE, Japan).

TOF-SIMS measurements

TOF-SIMS measurements were performed using a TRIFT III (ULVAC-PHI, Japan) spectrometer operating with a 22 keV Au_1^+ primary ion beam, a current of 1 nA and a pulse width of 15 ns. The primary ion beam was rastered over a hair cross-section of 125 × 125 μm area for visualizing the distribution of tripalmitin-d_{98}. A low-energy pulsed electron gun (28.0 eV) was used for surface charge compensation.

3.3. Results and Discussion

Figure 3.2 shows the inhibitory effect of conditioners on swelling of damaged hair. The results showed that the conditioner containing hydrogenated palm oil had greater inhibitory effect on swelling than control conditioner.

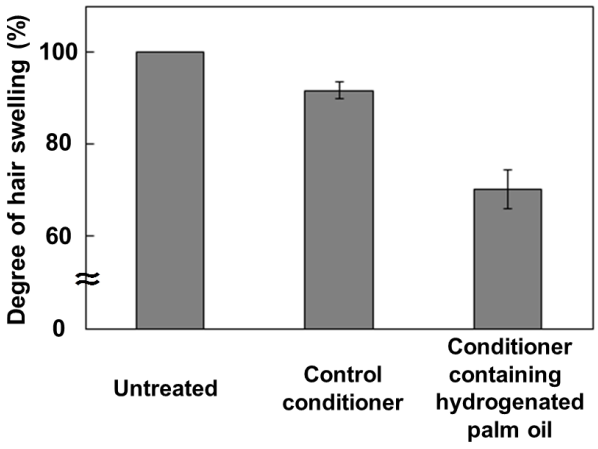

Figure 3.2 Inhibitory effect of conditioners on swelling of damaged hair.

The gas chromatogram of hydrogenated palm oil showed that four peaks were

mainly detected, and one of them was tripalmitin (Figure 3.3(a) and (b)). It was reported that molecular weight of the ingredient affects the sorption of the ingredient on hair [Naito et al., 1987]. Tripalmitin, which had a lowest molecular weight among the four peak components, was used as an indicator of hydrogenated palm oil because higher sorption on hair than other triglycerides was expected. First, I examined the damaged hair treated with a conditioner containing tripalmitin. Tripalmitin was clearly detected from the extract of hair treated with a conditioner containing it, in contrast with the extract of hair treated with the control conditioner (Figure 3.3(c) and (d)).

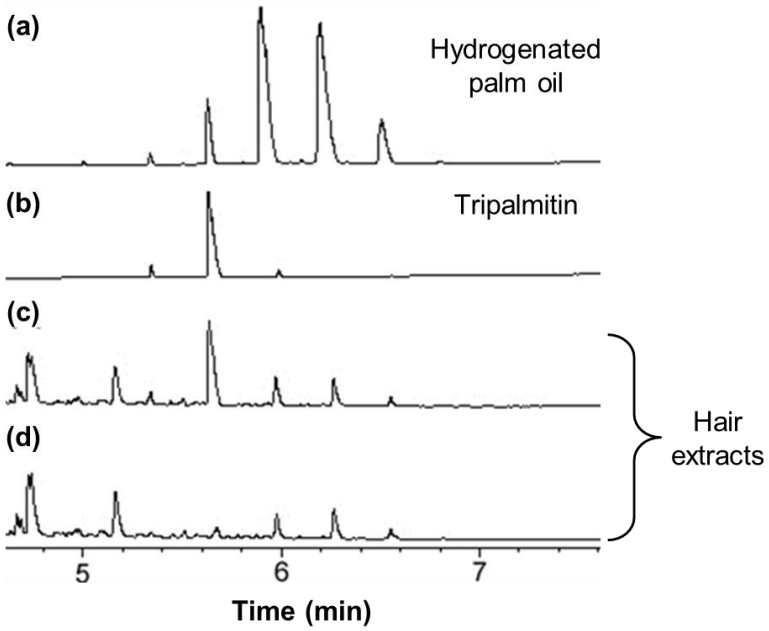

Figure 3.3 Gas chromatograms: (a) hydrogenated palm oil and (b) tripalmitin; extract of hair treated with (c) conditioner containing tripalmitin and (d) control conditioner.

However, fragment ion peaks derived from tripalmitin could not be detected in the positive and negative TOF-SIMS spectra of hair cross-section. Therefore, deuterium-labeled tripalmitin, tripalmitin-d_{98}, was used because a deuterium-labeled organic compound efficiently improves the sensitivity of TOF-SIMS analysis. Moreover, deuterium ion can be used as a characteristic fragment ion peak of its organic compound [Chapter 2]. Figure 3.4 shows the negative TOF-SIMS spectra of tripalmitin and tripalmitin-d_{98}. The spectrum of tripalmitin-d_{98} shows that the peak of the deuterium ion at *m/z* 2 was detected as the most intense fragment ion peak, and the fragment ion at *m/z* 286 derived from palmitic acid in the chemical structure of tripalmitin-d_{98} was also

detected.

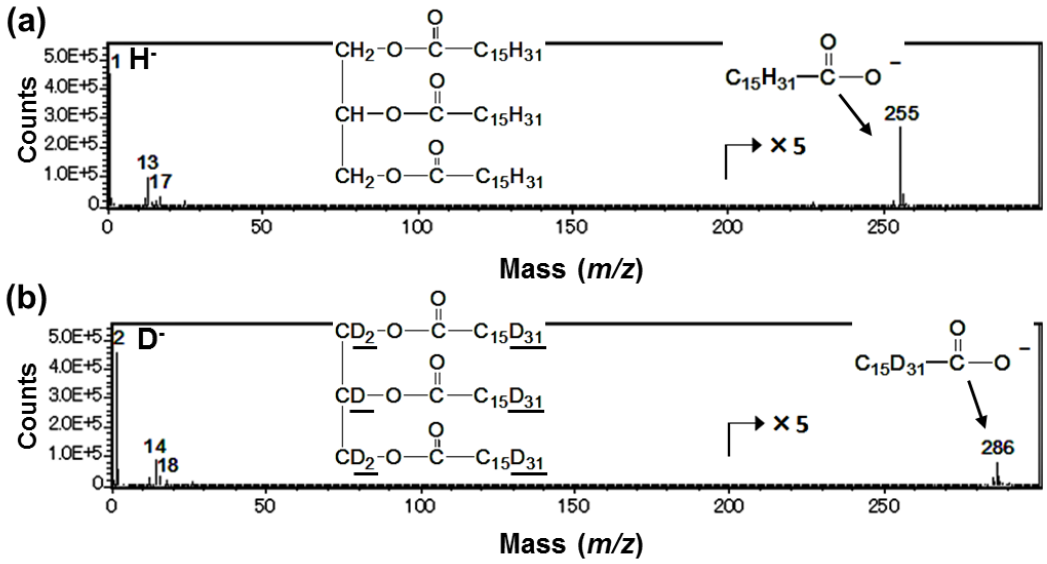

Figure 3.4 Negative TOF-SIMS spectra (*m/z* = 0–300): (a) tripalmitin, (b) tripalmitin-d_{98}.

Further, deuterium ion peak was clearly observed in the negative TOF-SIMS spectrum of the cross-section of damaged hair treated with a conditioner containing tripalmitin-d_{98}, as opposed to the spectrum of the cross-section of damaged hair treated with the control conditioner (Figure 3.5).

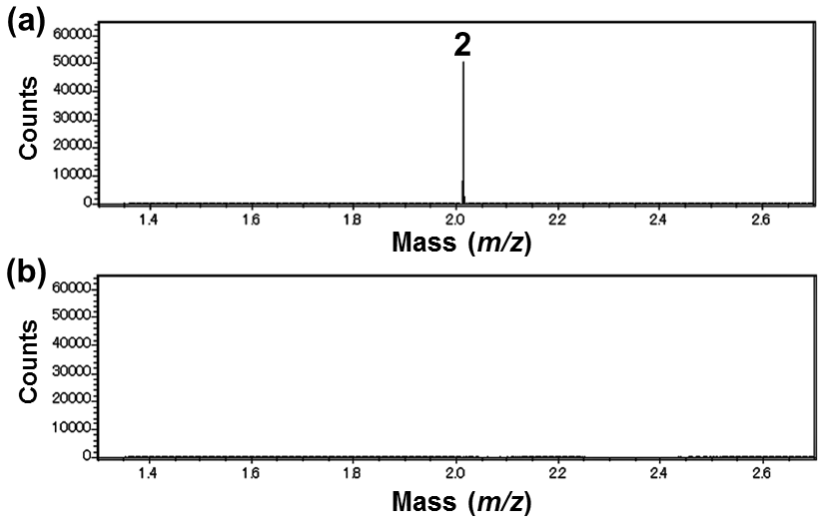

Figure 3.5 Negative TOF-SIMS spectra (*m/z* = 1.3–2.7) of the damaged hair cross-section treated with (a) conditioner containing tripalmitin-d_{98} and (b) control conditioner.

From the results of Figures 3.3–3.5, it is considered that deuterium ion detected from the hair cross-section was a fragment ion derived from tripalmitin-d_{98} penetrating into the hair. Deuterium ion mapping was carried out to estimate the penetration of tripalmitin-d_{98} (Figure 3.6). It was confirmed that tripalmitin-d_{98} penetrated into damaged hair and localized around the perimeter (Figure 3.6(a) and (b)). The line profile of TOF-SIMS ion mapping indicated that the degree of penetration of tripalmitin-d_{98} was approximately 10 μm from the hair surface (Figure 3.6(c)). On the other hand, the LSM image of the cross-section of the damaged hair treated with conditioner containing tripalmitin-d_{98} after TOF-SIMS analysis indicated that the thickness of the cuticle was approximately 4 μm (Figure 3.6(d)).

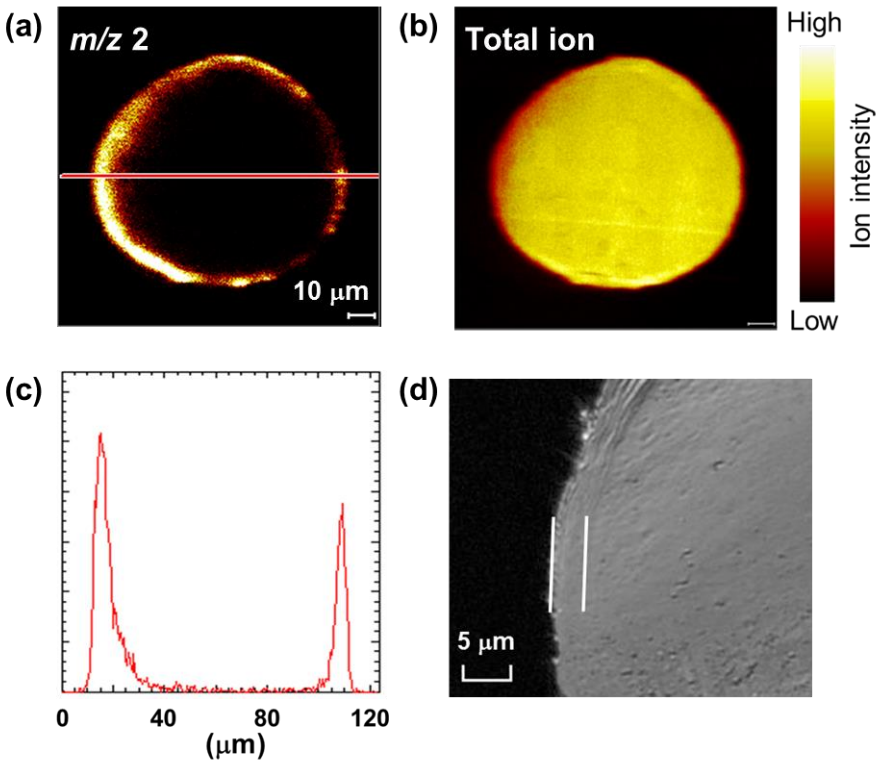

Figure 3.6 TOF-SIMS negative ion images, TOF-SIMS line profile, and LSM image of the damaged hair cross-section treated with conditioner containing tripalmitin-d_{98}: (a) and (b) TOF-SIMS ion images; (a) deuterium ion (m/z = 2) image, (b) total ion image; (c) TOF-SIMS line scan direction is indicated with line in (a); and (d) LSM image after TOF-SIMS analysis.

Results of TOF-SIMS ion mapping combined with that of LSM image revealed that tripalmitin-d_{98} penetrated into the cuticle and the outer cortex of damaged hair. It was reported that ortho-type cortical cells existed in the region of the outer cortex adjacent to the cuticle [Kassenbeck, 1981] and suffered greater damage because of bleaching than the internal cortical cells [Kitano et al., 2008]. Therefore, it is suggested that the great inhibitory effect on swelling by hydrogenated palm oil containing tripalmitin was due to its penetration into the cuticle and outer cortex of damaged hair, which suffered greater damage than the internal cortical cells.

3.4. Summary

Hydrogenated palm oil was shown to have a substantial effect on the repair of damaged hair. The penetration of tripalmitin, which is contained in hydrogenated palm oil, into damaged hair was investigated by TOF-SIMS. The TOF-SIMS images suggested that the effective inhibition of swelling by hydrogenated palm oil was due to its penetration into and localization in the cuticle and outer cortex of damaged hair.

Chapter 4
Compositional changes of human hair melanin resulting from bleach treatment investigated by nanoscale secondary ion mass spectrometry (NanoSIMS)

4.1. Introduction

Melanin, which is contained in human skin and hair, is a polymeric pigment with a complicated and heterogeneous structure [Prota, 1997; Riley, 1997; Ito et al., 2008; Robbins, 2012c]. Melanin is classified into two types: eumelanin, a dark brown-to-black pigment, and pheomelanin, a yellow-to-reddish brown pigment. The natural hair color is considerably different among races. Various natural hair colors are generated because of the differences in melanin content and the ratio of eumelanin and pheomelanin [Borgers et al., 2001; Ito et al., 2011]. Most of the melanin granules in the hair are located in the cortex [Imai, 2011; Marsh et al., 2012]. Although the complete chemical structure of melanin has not yet been elucidated, its partial structure has been described. The indole quinone and the dihydroxyindole units are contained as major repeating structural units in eumelanin (Figure 4.1) [Prota, 1997; Riley, 1997; Ito et al., 2008; Robbins, 2012c].

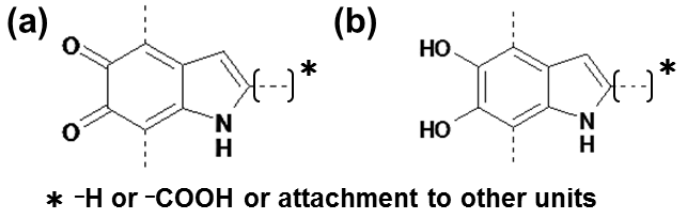

Figure 4.1 Major repeating units contained in eumelanin structure: (a) an indole quinone unit and (b) a dihydroxyindole unit [Prota, 1997; Riley, 1997; Ito et al., 2008; Robbins, 2012c].

Bleaching products are widely used to lighten the original hair color by decolorizing the melanin in hair [Wolfram et al., 1970; Brown, 1997; Marsh, 2012; Robbins, 2012c]. Bleaching mechanism is the partial oxidative degradation of melanin

structure by alkaline hydrogen peroxide. The oxidative hair coloring products also have a bleaching effect similar to the bleaching products. Thus, bleach treatment is one of the most important chemical treatments in hair cosmetic processes. Therefore, it is important to understand in detail the influences of bleach treatment on human hair.

It has not been clarified in detail how chemical treatments influence the chemical structure of melanin because melanin is a nanometer-sized insoluble polymeric pigment with a complex structure. The bleach treatment causes partial oxidative degradation of melanin granules and lightens color of the hair. Previous studies have proposed the degradative reactions of eumelanin by bleach treatment (Figure 4.2) [Slawinska et al., 1982; Korytowski et al., 1990; Marsh, 2012; Robbins, 2012c]. It is expected from these reactions that the structural changes of melanin by bleaching affect its elemental composition. Therefore, comparison of the elemental composition of melanin in virgin hair and bleached hair would provide important information about the structural changes of melanin. The characterization of melanin granules is generally performed after isolating them from hair [Sakamoto et al., 1978; Arnaud et al., 1981; Menon et al., 1983; Zvaik et al., 1986; Liu et al., 2003]. However, melanin isolation methods which often use acid/base extraction may affect the chemical composition of melanin. In addition, it is difficult to compare the chemical compositions of the melanin granules isolated from virgin hair and bleached hair because a part of melanin in bleached hair dissolves in extraction solution [Wolfram et al., 1970; Takada et al., 2003]. Therefore, to investigate the elemental composition of melanin without isolating it from the hair, techniques that can directly analyze melanin are required.

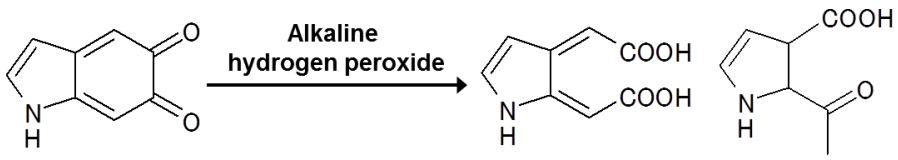

Figure 4.2 Proposed reactions for degradation of eumelanin by bleach treatment [Slawinska et al., 1982; Korytowski et al., 1990; Marsh, 2012; Robbins, 2012c]

In this chapter, to investigate the differences in the elemental composition of melanin granules in virgin black hair and bleached hair, the hair cross-sections were analyzed by NanoSIMS.

4.2. Materials and Methods

Materials

I used Japanese virgin black hair, which had never been chemically treated and was collected approximately 5 cm from the root. 25 wt% ammonia solution (Wako Pure Chemical Industries, Japan) and 30 wt% hydrogen peroxide (Wako Pure Chemical Industries, Japan) were used without further purification.

Bleaching treatment

Bleaching treatment was performed for 40 min at 30°C in a mixture that contained 2 wt% ammonia aqueous solution and 6 wt% hydrogen peroxide aqueous solution, which were mixed prior to use. After bleaching, the hairs were rinsed with purified water and dried with a hair dryer. This procedure of bleaching treatment was repeated three times; these hairs were called bleached hair.

Optical microscopy measurements

The virgin black hair and bleached hair were placed between celluloid plates and approximately 10 μm thick sections of hair samples were prepared using a microtome (ERM-230L.C, ERMA INC., Japan). These sections were observed using an optical microscope.

NanoSIMS measurement

The virgin black hair and bleached hair samples, which were used for the NanoSIMS measurement, were prepared from the same specimen. These hairs were embedded in epoxy resin together and extremely smooth hair cross-sections were obtained using an ultramicrotome (EM-ULTRACUT UCT, Leica Microsystems GmbH, Germany) equipped with a diamond knife. NanoSIMS 50L (Cameca, France) measurements were performed using a 16 keV Cs^+ primary ion beam to detect negative

secondary ions. The primary ion current was 1.7 pA. To reduce the charging effect, a thin gold layer was deposited on the sample surface. Ion images of 55 × 55 μm were recorded in 512 × 512 pixels with an acquisition time of 5 ms per pixel. Two images were continuously measured and the images were superimposed.

LSM measurements

LSM measurements of hair cross-sections were performed using VK-8710 laser scanning microscope (KEYENCE, Japan).

4.3. Results and Discussion

Macroscopic changes of the hair resulting from bleach treatment

The color of virgin black hair was lightened by bleach treatment. Figure 4.3 shows the optical microscopy images of hair cross-sections. The color of melanin granules in bleached hair is light brown, whereas that in virgin hair is black (Figure 4.3). Thus, melanin granules were decolorized by bleach treatment using alkaline hydrogen peroxide.

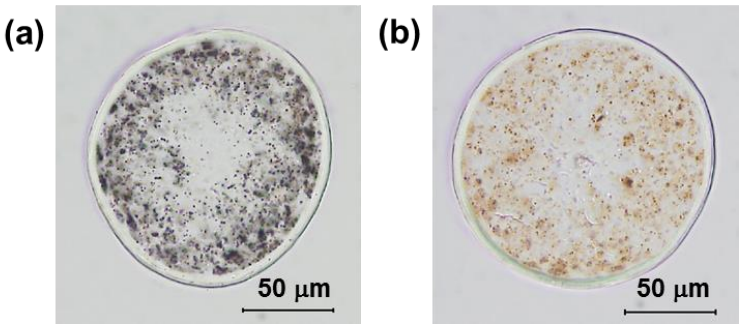

Figure 4.3 Optical microscopy images of hair cross-sections: (a) virgin black hair and (b) bleached hair.

Compositional changes of hair melanin resulting from bleach treatment

Figure 4.4 shows the NanoSIMS $^{16}O^-$ ion image of the hair cross-sections. The $^{16}O^-$ ions were intensely detected from several hundred nanometer-sized particulate regions in the cortex of both virgin black hair and bleached hair (Figure 4.4). The LSM images of the cross-sections of virgin black hair before and after the NanoSIMS measurement are shown in Figure 4.5. The surface of the hair cross-section was sputtered by irradiation of continuous primary ion beam during the NanoSIMS measurement (Figure 4.5). The particulate patterns were observed in cortex (Figure 4.5 (b)). Those positions agreed well with the positions of the particulate regions where $^{16}O^-$ ions were intensely detected in the NanoSIMS image (Figure 4.4 and 4.5 (b)). In previous studies using argon sputter etching-SEM (ASE-SEM), melanin granules were observed as particulate patterns [Masukawa et al., 2005 and 2006]. The particulate patterns observed in this chapter are similar to those observed in the ASE-SEM images of hair cross-sections (Figure 4.5 (b)). Furthermore, it was indicated in a previous study using NanoSIMS that melanin granules are oxygen-rich tissue [Hallegot et al., 2004]. On the basis of my findings shown in Figures 4.4 and 4.5, the particulate regions, where $^{16}O^-$ ions were intensely detected in the NanoSIMS image, were identified as melanin granules.

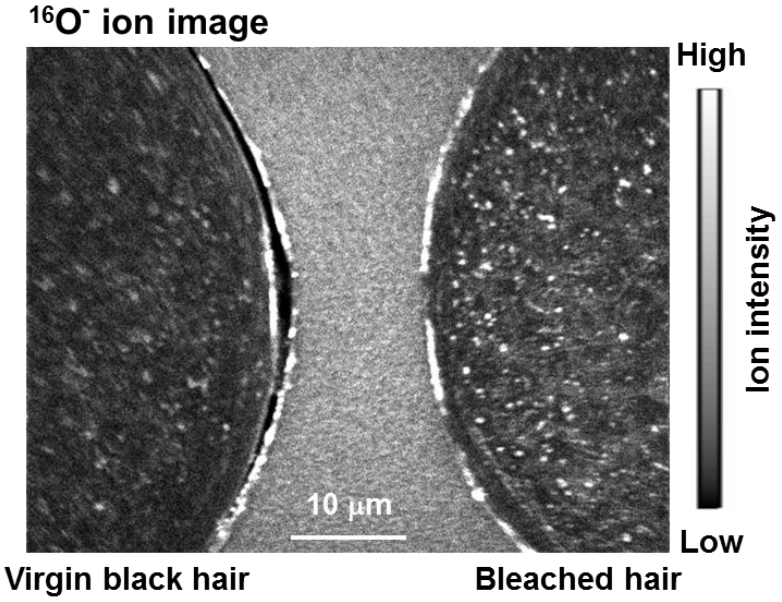

Figure 4.4 NanoSIMS $^{16}O^-$ ion image of hair cross-sections.

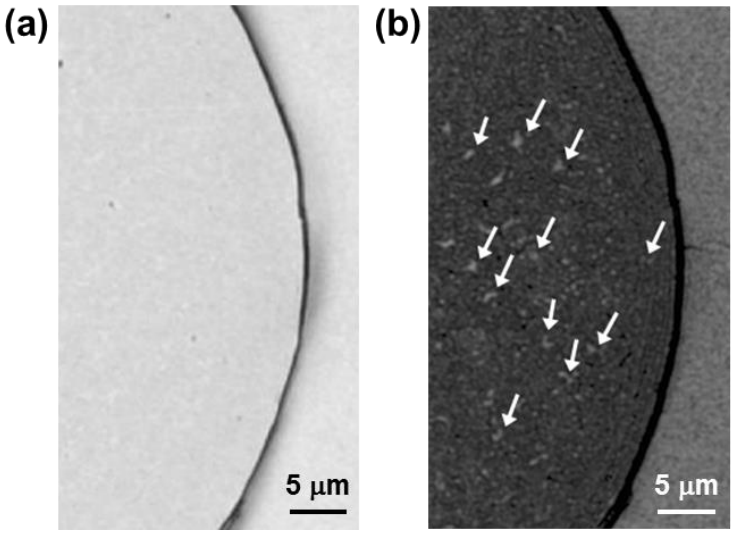

Figure 4.5 LSM images of the cross-sections of virgin black hair before (a) and after (b) NanoSIMS measurement. Arrows: typical particulate patterns.

When the NanoSIMS $^{16}O^-$ ion images of virgin black hair and bleached hair were compared, more intensive $^{16}O^-$ ions were detected from the melanin granules of bleached hair than from those of virgin black hair (Figure 4.4). In addition, 25 particulate regions, where $^{16}O^-$ ions were intensely detected in the NanoSIMS image, were chosen from virgin black hair and bleached hair, respectively. The ion intensity values of these regions were calculated and data analysis was performed using those values. Figure 4.6 shows the $^{16}O^-$ ion intensity and $^{16}O^-/^{12}C^{14}N^-$ ion intensity ratio. The $^{12}C^{14}N^-$ ion was used in the ion intensity ratio because its ion is strongly detected in biological materials [Williams, 2006]. It was indicated that $^{16}O^-$ ion intensity and $^{16}O^-/^{12}C^{14}N^-$ ion intensity ratio of melanin granules in bleached hair were higher than those in virgin black hair (Figure 4.6). From the results of Figures 4.4 and 4.6, it was indicated that bleach treatment increased the oxygen content in melanin granules.

The most of melanin contained in the black hair is eumelanin [Borgers et al., 2001; Ito et al., 2011]. In proposed reactions for degradation of eumelanin (Figure 4.2) [Slawinska et al., 1982; Korytowski et al., 1990; Marsh, 2012; Robbins, 2012c], the oxygen content in the chemical structure of eumelanin increases because of the ring-opening of the indole quinone unit in eumelanin by bleaching. Therefore, it is considered that the results of NanoSIMS analysis reflect the influence of bleach treatment on the chemical structure of melanin.

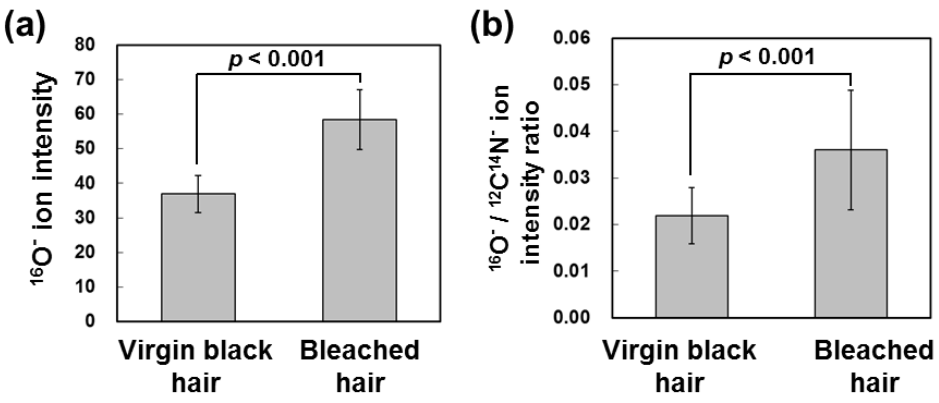

Figure 4.6 Data analysis of the particulate regions where $^{16}O^-$ ions were strongly detected in the NanoSIMS image: (a) $^{16}O^-$ ion intensity and (b) $^{16}O^-/^{12}C^{14}N^-$ ion intensity ratio. The ion intensity values are the average ion counts per pixel in the particulate regions.

4.4. Summary

NanoSIMS analysis of the cross-sections of virgin black hair and bleached hair indicated that the oxygen content in melanin granules was increased by bleach treatment. By the NanoSIMS elemental mapping, I observed that bleaching resulted in a change in the elemental composition of melanin, which is one of the fine structures of the hair.

Chapter 5
Dyeing regions of oxidative hair dyes in human hair investigated by nanoscale secondary ion mass spectrometry (NanoSIMS)

5.1. Introduction

Optical microscopy is useful for showing that the oxidative hair dyeing actually occurs in the cuticle and the cortex [Wilmsman, 1961; Imai et al., 2008]. However, it is difficult to observe the distribution and localization of the colored chromophores formed from oxidative dyes in the fine structure of hair. Additionally, fluorometric techniques having high spatial resolution, such as CLSM and SNOM, cannot be used to evaluate oxidative dyeing because colored chromophores formed from oxidative dyes are not fluorescent. Therefore, it is difficult to investigate dyeing regions of oxidative coloring in the fine structure of hair by using conventional techniques. To develop more effective oxidative hair coloring product and hair care product for maintaining colored hair, it is important to understand the localization of colored chromophores in the fine structure of hair.

In this chapter, the distribution and localization of the colored chromophores formed from oxidative dyes in the fine structure of human hair were investigated by using a stable isotope-labeled oxidative dye with NanoSIMS.

5.2. Materials and Methods

Materials

I used virgin black human hair, which had never been damaged by any chemical treatments such as bleaching, hair coloring, and permanent waving. Three sample sets of black and white hair were obtained from three Japanese (Samples 1-3).

I used *p*-phenylenediamine (pPD; Nacalai Tesque, Japan), 1,4-phenylenediamine-2,3,5,6-d_4 (pPD-d4; C/D/N Isotopes Inc., Canada), which is a deuterium-labeled

oxidative hair dye; 5-amino-*o*-cresol (pAOC; Tokyo Chemical Industry, Japan), 25wt% ammonia solution (Wako Pure Chemical Industries, Japan), 30wt% hydrogen peroxide (Wako Pure Chemical Industries, Japan), ascorbic acid (Sigma-Aldrich Japan, Japan), and methanol (Wako Pure Chemical Industries, Japan) without further purification.

Oxidative dyeing and bleaching treatments

Colorant aqueous solutions contained 0.08 M of pPD or pPD-d4, 0.08 M of pAOC, 2 wt% ammonia, and 0.1 wt% ascorbic acid. The colorant aqueous solution without oxidative dye was used for bleaching. The developer aqueous solution contained 6 wt% hydrogen peroxide. The colorant and developer were mixed just before use. Next, the mixture was applied to hair samples and left for 60 min at 30°C. After dyeing, the hairs were rinsed with purified water and dried using a hair dryer.

Extraction of colored chromophores from hair samples [Imai et al., 2010]

Dyed hair samples were powdered by frost shattering (Freezer/Mill 6750; SPEX, America) or by using a glass homogenizer. Colored chromophores in hair powder (10 mg) were extracted in methanol (5mL) under ultrasonic conditions for 30 min.

Visible spectra

Visible spectra of methanol extracts were measured using a UV-2450 UV-visible spectrometer (Shimadzu Corporation, Japan).

TOF-SIMS measurements

Methanol extracts were dropped onto a Si wafer and dried. The wafers were then analyzed using TOF-SIMS. TOF-SIMS measurements were performed using a TRIFT III spectrometer (ULVAC-PHI, Japan). Positive spectra were obtained using a 22 keV Au_1^+ primary ion beam at a current of 1 nA. A low-energy pulsed electron gun was used for surface charge compensation.

NanoSIMS measurements

Dyed hairs were embedded in epoxy resin, and made smooth surface of the hair cross-section using an ultramicrotome (EM-ULTRACUT UCT, Leica Microsystems GmbH, Germany) equipped with a diamond knife. NanoSIMS 50 (Cameca, France) measurements were performed using a 16 keV Cs^+ primary ion beam, operating at a current of 0.8–1.0 pA, to detect negative secondary ions. To reduce the charging effect, a thin gold layer was deposited on the sample surface and an electron gun was used. NanoSIMS images were recorded in 256 × 256 pixels.

5.3. Results and Discussion

Colored chromophores extracted from dyed hair

Figure 5.1 shows visible spectra of methanol extracts obtained from dyed hairs and bleached hair. The visible spectra of the methanol extract obtained from hair dyed with pPD-d4 and pAOC showed equivalent visible adsorption when compared with those obtained from the hair dyed with pPD and pAOC (Figure 5.1(a) and (b)). Visible adsorption was hardly detected on the spectrum for the bleached hair (Figure 5.1(c)). These results indicate that pPD-d4 reacts to pAOC in a manner very similar to pPD.

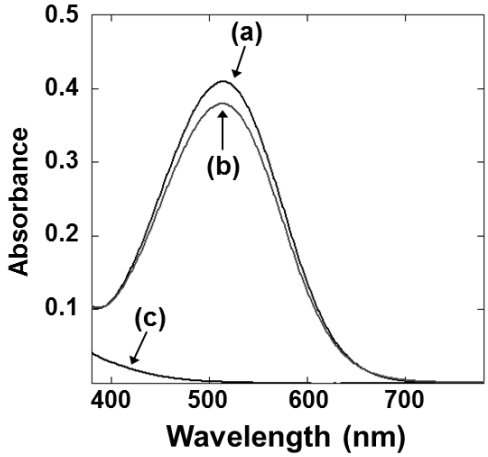

Figure 5.1 Visible spectra of methanol extracts obtained from dyed hairs and bleached hair: (a) pPD and pAOC, (b) pPD-d4 and pAOC, and (c) bleached hair.

Previous studies reported that oxidative dyeing of pPD and pAOC mainly produced binuclear indo dye, 2-amino-5-methylindoaniline (2A5MIA) (Figure 5.2) [Corbett, 1973; Pillai et al., 2005]. Figure 5.3 shows positive TOF-SIMS spectra of extracts obtained from dyed hair and bleached hair. For the extracts obtained from bleached hair, the positive TOF-SIMS spectrum showed no clear ion peaks at higher than *m/z* 200 (Figure 5.3(c)). However, an ion peak at *m/z* 228, corresponding to the molecular ion peak of $[2A5MIA + H]^+$ formed from pPD and pAOC, was detected on the positive TOF-SIMS spectrum (Figure 5.3(a)). Further, Figure 5.3(b) shows an ion peak at *m/z* 232, corresponding to deuterium-labeled 2A5MIA formed from pPD-d4 and pAOC. Therefore, the deuterium ion can be used as a characteristic fragment ion for the colored chromophore formed from pPD-d4 and pAOC.

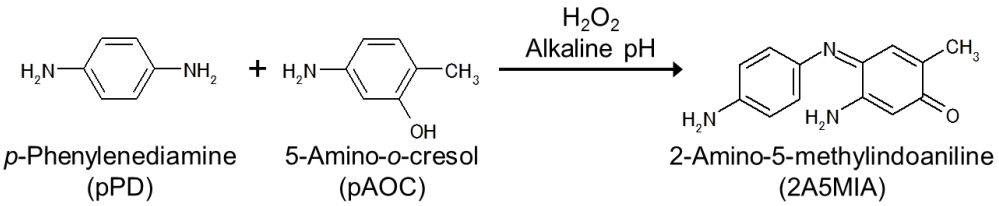

Figure 5.2 Binuclear indo dye formed from pPD and pAOC in oxidative dyeing [Corbett, 1973; Pillai et al., 2005].

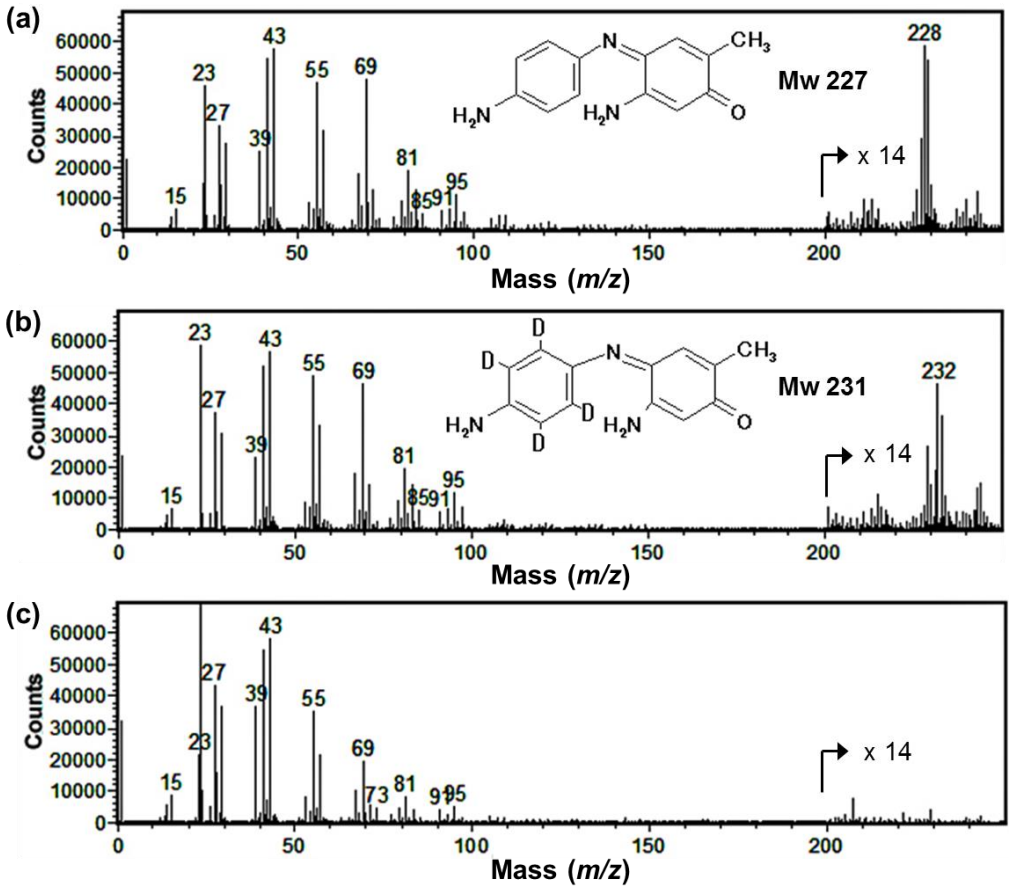

Figure 5.3 Positive TOF-SIMS spectra of extracts obtained from the dyed hairs and bleached hair (*m/z* = 0–250): (a) pPD and pAOC, (b) pPD-d4 and pAOC, and (c) bleached hair.

The NanoSIMS measurements of dyed and bleached hair

Figure 5.4 shows NanoSIMS images of cross-sections of hair dyed with pPD-d4 and pAOC and bleached hair. Deuterium ion mapping was carried out to investigate the penetration and localization of colored chromophores in hair. Although deuterium ions were detected in whole cross-section of dyed hair, they were more intensely detected in nano-sized particulate regions of hair, whereas they were hardly detected in the bleached hair (Figure 5.4(b) (c) (e) and (f)). As a result, colored chromophores are frequently formed in particulate constituents of black hair compared to others.

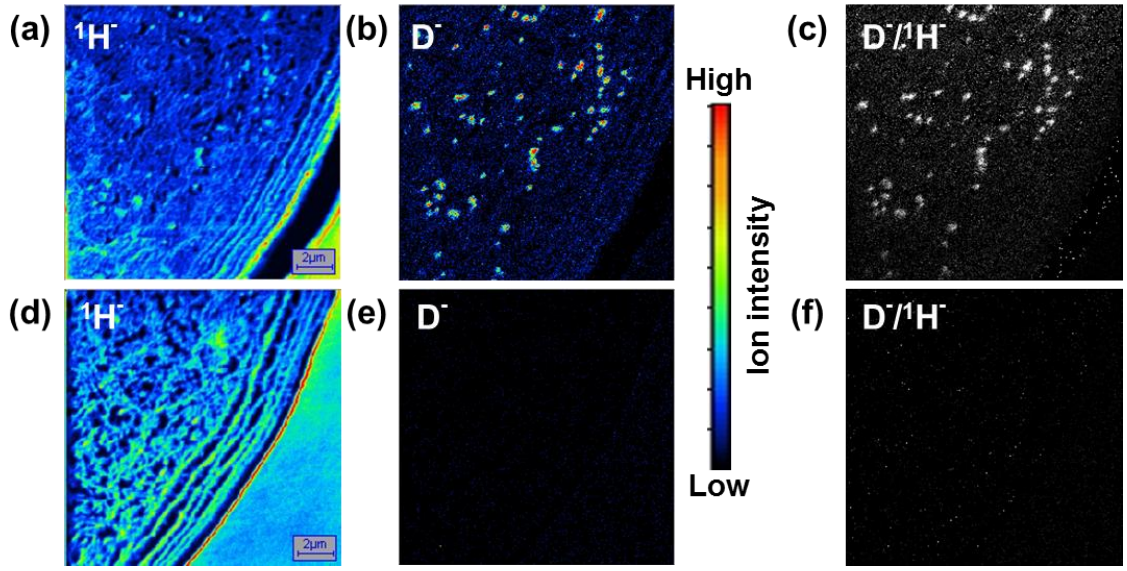

Figure 5.4 NanoSIMS images of the hair cross-section: (a)–(c) the hair dyed with pPD-d4 and pAOC: (a) $^1H^-$ image, (b) D^- image, and (c) $D^-/^1H^-$ image; (d)–(f) bleached hair: (d) $^1H^-$ image, (e) D^- image and (f) $D^-/^1H^-$ image.

Comparison of dyeing behavior of black and white hair in the same person

Figure 5.5 shows visible spectra of methanol extracts obtained from the black and white hair (sample 1) dyed with pPD and pAOC. Visible spectrum for both black and white hair showed absorbance at approximately 510 nm (Figure 5.5). This indicates that color formation is equivalent in the black and white hair. Table 5.1 shows absorbance values of methanol extracts obtained from dyed black and white hair at 510 nm. All hair samples indicate that methanol extracts of dyed black hair have higher absorbance values than those of dyed white hair. In a previous study using pPD and resorcinol as oxidative dyes, results similar to those seen in this study were reported [Imai et al., 2010]. Figure 5.5 and Table 5.1 show that more colored chromophores were generated in black hair than in white hair.

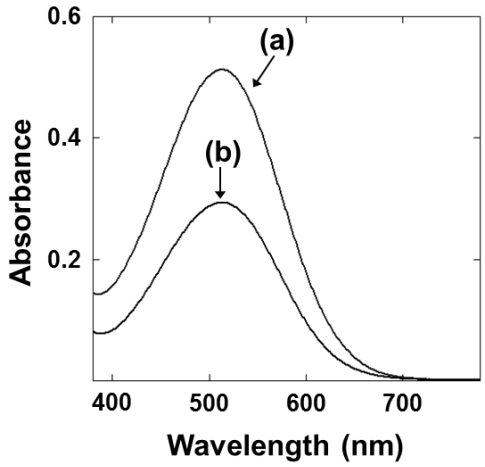

Figure 5.5 Visible spectra of methanol extracts obtained from the hair dyed with pPD and pAOC: (a) black hair and (b) white hair.

Table 5.1 510 nm absorbance values of methanol extracts obtained from the black and white hair dyed with pPD and pAOC.

	Black hair	White hair	Black hair / White hair
Sample1	0.51	0.29	1.76
Sample2	0.52	0.32	1.63
Sample3	0.45	0.40	1.13

Figure 5.6 shows NanoSIMS images of cross-sections of black and white hair dyed with pPD-d4 and pAOC. Deuterium ions were detected in whole hair cross-section, and more intensely detected from particulate regions in dyed black hair (Figure 5.6(b) and (c)). In dyed white hair, deuterium ions were detected from in whole hair cross-section (Figure 5.6(e) and (f)). However, particulate regions such as those confirmed in dyed black hair were not observed in dyed white hair. White hair hardly contains melanin granules compared to black hair. Additionally, the size and location of particulate region, where deuterium ions were intensely detected in dyed black hair, agree well with those of melanin granule. On the basis of the results shown in Figures 5.4–5.6 and Table 5.1, particulate regions in which deuterium ions were intensely detected in the dyed black hair were identified as melanin granules. Metal elements existing in black hair mainly localized in melanin granules [Watanabe et al., 1994; Imai et al., 2010], and trace transition metals accelerated the chromogenic reaction of oxidative dyes [Imai et al.,

2010]. Also, most of melanin granules did not elute from the hair by oxidative coloring although some parts of melanin structure were degraded [Imai, 2011]. Therefore, it is considered that more colored chromophores were formed in melanin granules than in other hair regions because of the high transition metal content.

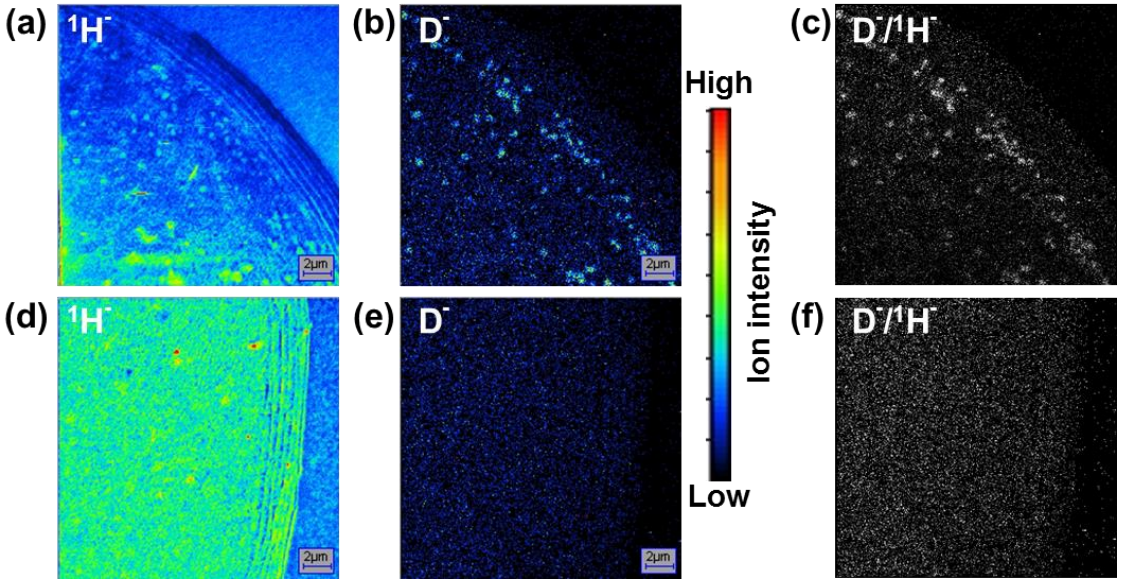

Figure 5.6 NanoSIMS images of the cross-section of the hair dyed with pPD-d4 and pAOC: (a)–(c) the dyed black hair: (a) $^1H^-$ image, (b) D^- image and (c) $D^-/^1H^-$ image; (d)–(f) the dyed white hair: (d) $^1H^-$ image, (e) D^- image and (f) $D^-/^1H^-$ image.

5.4. Summary

The NanoSIMS ion mapping images of deuterium ions on the cross-section of hair dyed with deuterium-labeled oxidative dye revealed that colored chromophores are intensely localized in melanin granules, where more trace transition metals are present. Therefore, melanin granules are important dyeing regions for oxidative hair coloring.

Chapter 6
Investigation of dyeing behavior of oxidative dye in fine structures of the human hair cuticle by nanoscale secondary ion mass spectrometry (NanoSIMS)

6.1. Introduction

The cuticle is the outermost tissue of the hair where the all hair treatments are first applied, and it is penetration pathway of the cosmetic ingredients into the hair interior [Naito et al., 1992; Wortmann et al., 1997; Gummer, 2001]. The active ingredients of chemical treatments, such as bleaching and hair coloring, penetrate the hair through the cuticle layers and act in the hair fiber. In oxidative hair coloring, the cuticle layers of human hair are not only the penetration pathway for active ingredients but also one of the most important dyeing regions. Considering the different cystine contents of the fine structures of cuticle, it is reasonable to assume that dyeing behavior differs among the fine structures of the cuticle. However, the dyeing behavior of oxidative dye in the fine structures of the cuticle is not confirmed because the fine structure of cuticle cannot be observed by optical microscopy and the location of dyes cannot be evaluated by conventional techniques for observing the hair structure such as SEM and TEM.

In Chapter 5, it was revealed by using deuterium-labeled oxidative dye with NanoSIMS that more colored chromophores formed in melanin granules of hair than in other hair regions. However, dyeing behavior in fine structures of the cuticle could not be revealed.

In this chapter, to investigate the dyeing behavior of oxidative dyes in fine structures of the hair cuticle, I improved the hair cross-section preparation method used for NanoSIMS measurement, and the improved hair cross-sections were analyzed by NanoSIMS.

6.2. Materials and Methods

Materials

Japanese virgin black hairs, which had never been damaged by any chemical treatments, were collected. I used the circular hairs and collected them approximately 5 cm part from the root of the hairs.

I used *p*-phenylenediamine (pPD; Nacalai Tesque, Japan), 1,4-phenylenediamine-2,3,5,6-d_4 (pPD-d4; C/D/N Isotopes Inc., Canada), which is a stable isotope-labeled oxidative hair dye, 5-amino-*o*-cresol (pAOC; Tokyo Chemical Industry, Japan), 25 wt% ammonia solution (Wako Pure Chemical Industries, Japan), 30 wt% hydrogen peroxide (Wako Pure Chemical Industries, Japan), ascorbic acid (Sigma-Aldrich Japan, Japan), ethanol (Wako Pure Chemical Industries, Japan), and methanol (Wako Pure Chemical Industries, Japan) without further purification.

Oxidative coloring and bleaching treatments

Colorant aqueous solutions contained 0.14 M of pPD or pPD-d4, 0.14 M of pAOC, 2.5 wt% ammonia, 5 wt% ethanol, and 0.1 wt% ascorbic acid. The colorant aqueous solution without dye was used for bleaching. The developer aqueous solution contained 6 wt% hydrogen peroxide. Oxidative coloring and bleaching treatments were carried out by immersing the hairs in a mixture of colorant and developer aqueous solutions for 60 min at 35°C. After treatments, the hairs were rinsed with purified water and dried using a hair dryer. The dyed hairs, which were treated with oxidative coloring one or three times, were prepared. In addition the bleached hair, which was bleached three times, was prepared.

Extraction of colored chromophores from hair samples [Imai et al., 2010]

Dyed hairs were powdered using a glass homogenizer. Colored chromophores in 10 mg of hair powder were extracted in 5 mL methanol under ultrasonic conditions for 30 min.

Visible spectra

Visible spectra of methanol extracts were measured using a UV-2450 UV-visible spectrometer (Shimadzu Corporation, Japan).

Electrospray ionization time-of-flight mass spectrometry (ESI-TOF-MS) measurements

Methanol extracts were diluted 200 times with methanol/water (90:10) (v/v). Those solutions were used for mass spectrometry. ESI-TOF-MS measurements were performed using a Mariner Biospectrometry Workstation (Applied Biosystems, California).

LSM measurements

The hairs were embedded in epoxy resin, and a smooth, cross-sectional surface of the hair was obtained using an ultramicrotome (EM-ULTRACUT UCT, Leica Microsystems GmbH, Germany) equipped with a diamond knife. LSM measurements of hair cross-sections were performed using a VK-8710 laser scanning microscope (KEYENCE, Japan).

Atomic force microscopy (AFM) measurement

An AFM measurement of a hair cross-section was performed using an EnviroScope equipped with a NanoScope IVa controller (Bruker AXS Inc., Wisconsin). A cantilever made of silicone (MPP-11100, Bruker AXS Inc., Wisconsin) was used and tapping-mode operation was performed.

NanoSIMS measurements

The dyed hair, which was oxidatively colored three times, and the bleached hair, which was bleached three times, were embedded in epoxy resin. Then, a smooth surface of the hair cross-section was obtained using an ultramicrotome (EM-ULTRACUT UCT, Leica Microsystems GmbH, Germany) equipped with a diamond knife. NanoSIMS 50 (Cameca, France) measurements were performed using a 16 keV Cs^+ primary ion beam to detect negative secondary ions. The primary ion current was 0.8–1.0 pA. The spatial resolution of approximately 100 nm (spot size) was expected under this measurement condition. To reduce the charging effect, a thin gold layer was deposited on the sample surface. NanoSIMS ion images were recorded in 256 × 256 pixels.

6.3. Results and Discussion

Analysis of colored chromophore extracted from dyed hair

Figure 6.1 shows the visible spectra of methanol extracts obtained from the dyed hairs. The absorption maximum wavelengths of all dyed hairs within the visible range were approximately 510 nm (Figure 6.1). When the visible spectra between the hairs dyed one and three times was compared, spectral shapes appeared similar, but the hair dyed three times had higher absorbance than the hair dyed once (Figure 6.1(a) and (b)). In addition, the visible spectrum of methanol extract from the hairs dyed with pPD-d4 and pAOC showed a spectral shape similar to that of the hairs dyed with pPD and pAOC (Figure 6.1(b) and (c)).

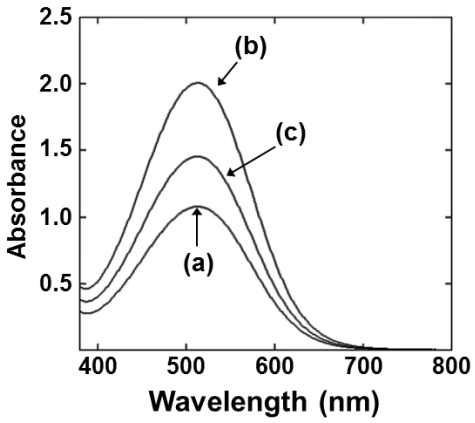

Figure 6.1 Visible spectra of methanol extracts obtained from dyed hairs: (a) and (b) the hair dyed with pPD and pAOC: (a) dyed one time, (b) dyed three times; and (c) the hair dyed with pPD-d4 and pAOC and dyed three times.

It was reported that binuclear indo dye, 2-amino-5-methylindoaniline (2A5MIA), was mainly formed in oxidative dyeing using pPD and pAOC (Figure 5.2) [Corbett, 1973; Pillai et al., 2005]. Figure 6.2 shows the positive ESI-TOF-MS spectra of extracts obtained from the dyed hairs. In the spectra of the hairs dyed with pPD and pAOC, an ion peak at *m/z* 228, corresponding to the molecular ion peak of $[2A5MIA+H]^+$ formed from pPD and pAOC, was detected (Figure 6.2(a) and (b)). From Figure 6.1(a)–(b) and Figure 6.2(a)–(b), it was indicated that the colored chromophores formed by dyeing three times were equivalent to dyeing once, and that more colored chromophores were formed in the hair dyed three times than the hair dyed once. Furthermore, an ion peak at *m/z* 232, corresponding to the molecular ion peak of [deuterium-labeled $2A5MIA+H]^+$ formed from pPD-d4 and pAOC, was detected (Figure. 6.2(c)). This indicates the formation of binuclear indo dye retaining deuterium in its chemical structure. Therefore, the deuterium ion can be used as a characteristic ion of the binuclear indo dye formed from pPD-d4 and pAOC.

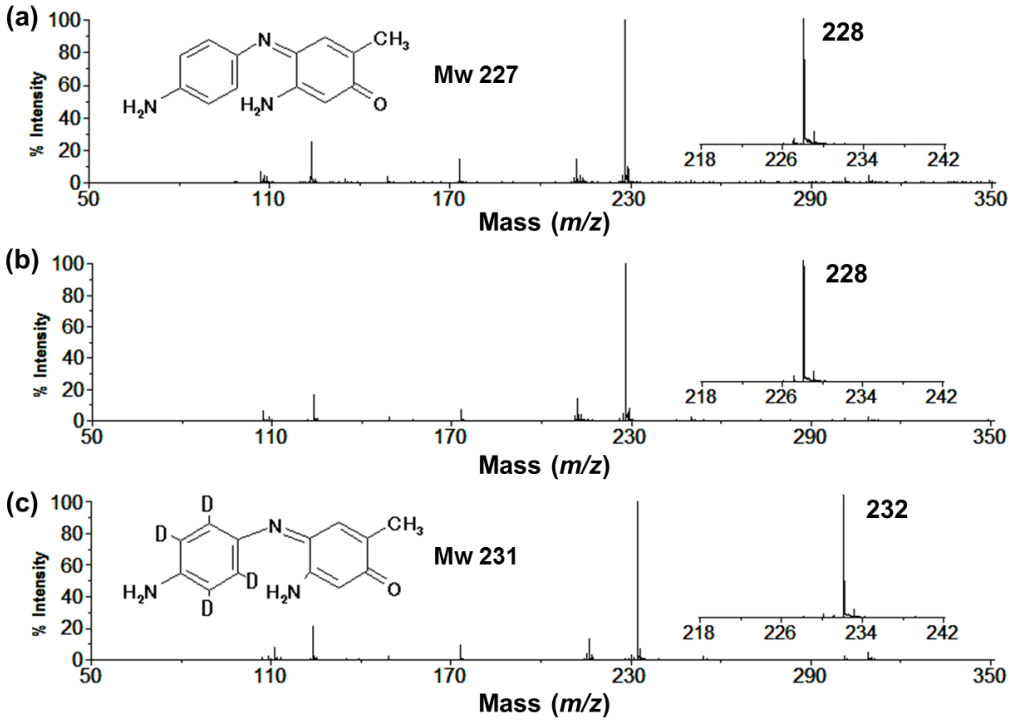

Figure 6.2 Positive ESI-TOF-MS spectra of extracts obtained from the dyed hairs (m/z = 50–350): (a) and (b) the hair dyed with pPD and pAOC: (a) dyed one time, (b) dyed three times; and (c) the hair dyed with pPD-d4 and pAOC and dyed three times.

Improvement of sample preparation of hair cross-section for NanoSIMS measurement

When the hair sample is embedded in the resin to prepare the hair cross-section, it has generally been placed perpendicular to the cutting surface. The thickness of cuticle layers in hair cross-section prepared from the resin of this state is untouched (Figure 6.3(a) and (b)). In the NanoSIMS analysis using the hair cross-sections made by general preparation method, dyeing behavior in the fine structures of the cuticle could not be revealed. This was attributed that spatial resolution of NanoSIMS in measurement condition having sensitivity for measuring colored chromophores in the hair was too close to the thickness of the fine structures of the hair cuticle. Therefore, I improved the sample preparation method of hair cross-section for NanoSIMS measurement. To widen the thickness of cuticle layers, the hair was embedded diagonally to the cutting surface and its cross-section was made. As a result, an elliptical, laterally widened hair

cross-section was obtained (Figure 6.3(c) and (d)). Figure 6.3 (e) shows an AFM height image of hair cross-section. AFM can observe the fine structures of hair under ambient conditions, such as in air and water [Chen et al., 2005; Kitano et al., 2009]. The widened cuticle layer thickness was approximately 1.5 μm and the fine structures of the cuticle were observed. As a result of improved sample preparation, the thickness of a cuticle layer in the hair cross-section was increased approximately three times.

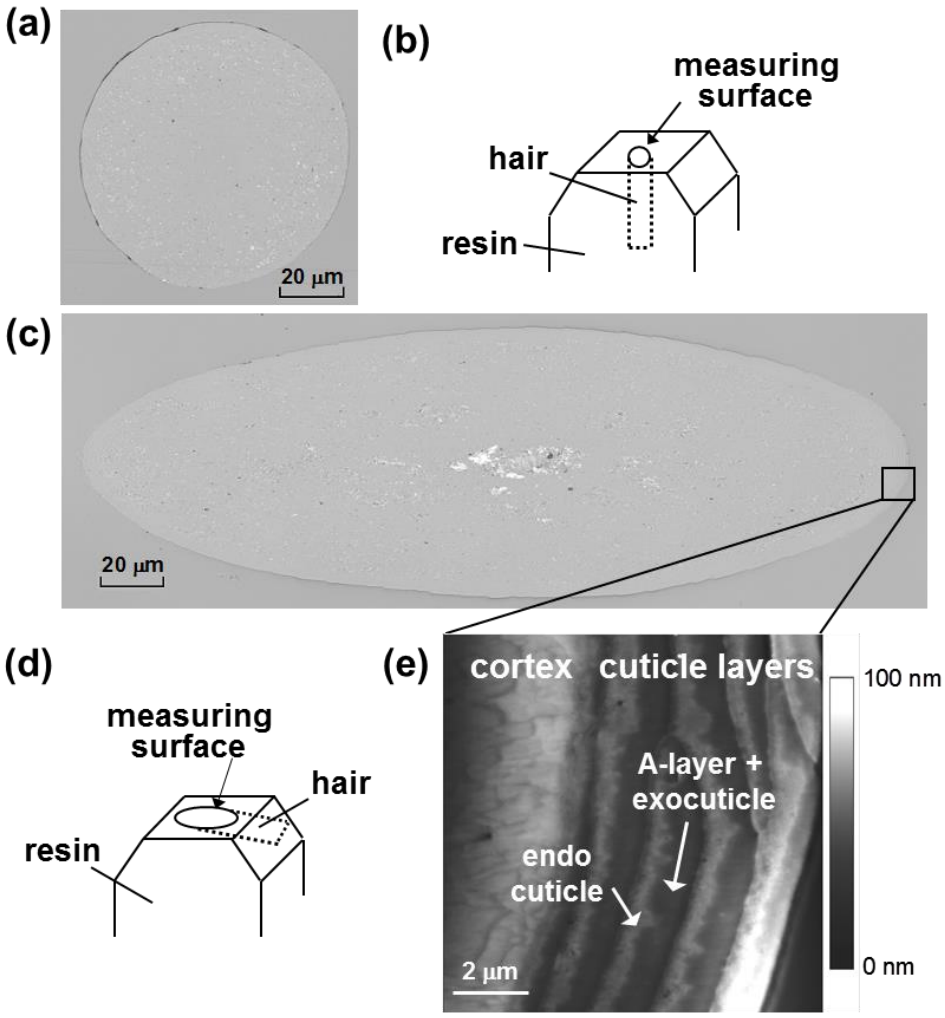

Figure 6.3 Preparation of hair cross-sections: (a) and (c) LSM images; (b) and (d) the schematic views of the hair embedded in the resin; and (e) AFM height image.

The NanoSIMS measurements

Figure 6.4 shows NanoSIMS images of the bleached hair cross-section. Deuterium

ions were hardly detected (Figure 6.4(b) and (d)). Focusing on the cuticle layers in the $^{12}C^-$ image, two layers were observed in a cuticle layer (Figure 6.4 (c)). By comparing the AFM image (Figure 6.3 (e)) and NanoSIMS $^{12}C^-$ image (Figure 6.4 (c)), I confirmed that $^{12}C^-$ ions were strongly detected from the cystine-poor region (endocuticle), in comparison with the cystine-rich regions (A-layer and exocuticle). In previous studies using NanoSIMS, the fine structures of the hair cuticle were identified by $^{12}C^-$ and $^{32}S^-$ images [Hallegot et al., 2004; Smart et al., 2009]. Therefore, NanoSIMS $^{12}C^-$ image of hair cross-section can be used for the identification of fine structures in a cuticle layer.

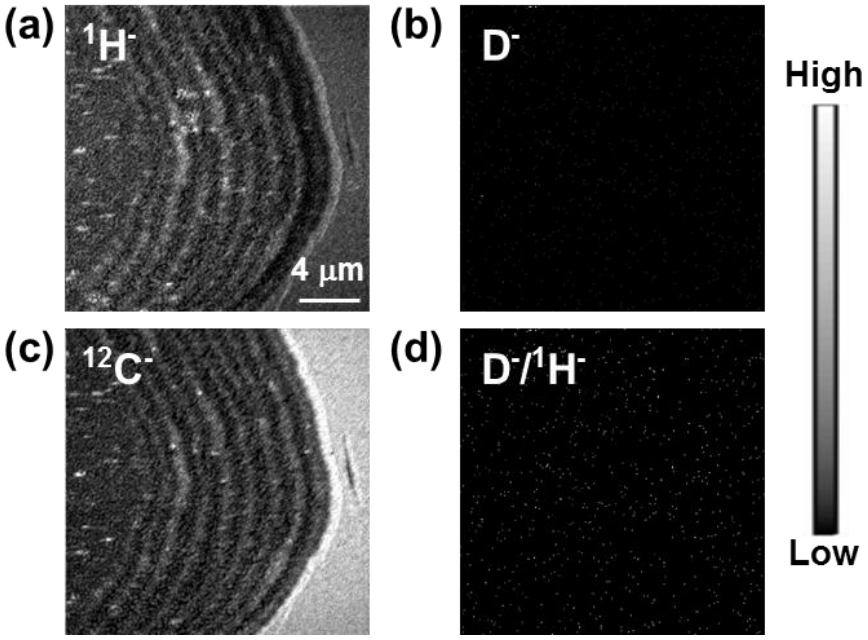

Figure 6.4 NanoSIMS images of the bleached hair cross-section: (a) $^1H^-$ image, (b) D^- image, (c) $^{12}C^-$ image, and (d) $D^-/^1H^-$ ratio image.

Figure 6.5 shows NanoSIMS images of cross-section of the hair dyed with pPD-d4 and pAOC. Deuterium ions were detected from the entire hair cross-section and they were intensely detected from granular regions in the cortex (Figure 6.4(b) and (d)). Their granular regions are melanin [Chapter 5]. Hue saturation intensity (HSI) transformation of $D^-/^1H^-$ ratio image was performed because it can visually increase the contrast of the isotope ratio data (Figure 6.5(e)) [Lechene et al., 2006; McMahon et al., 2006]. As a result, it was confirmed that the regions corresponding to the endocuticle, where high $^{12}C^-$ ions were detected, had a higher $D^-/^1H^-$ ratio than other fine structures

of the cuticle layer (Figure 6.5(c) and (e)). This indicates that the endocuticle is more dyed by oxidative dyeing than other fine structures of the cuticle layer. The endocuticle is composed of nonkeratinous protein with high water swellability [Swift, 1992]. Therefore, it is considered that oxidative dyes preferentially penetrate and diffuse in the endocuticle, and that the formation and fixation of colored chromophores are occurred in that region during oxidative dyeing. The NanoSIMS images of the dyed hair substantiated that more colored chromophores formed by oxidative dyeing were fixated in the endocuticle than in the other fine structures of the cuticle layer.

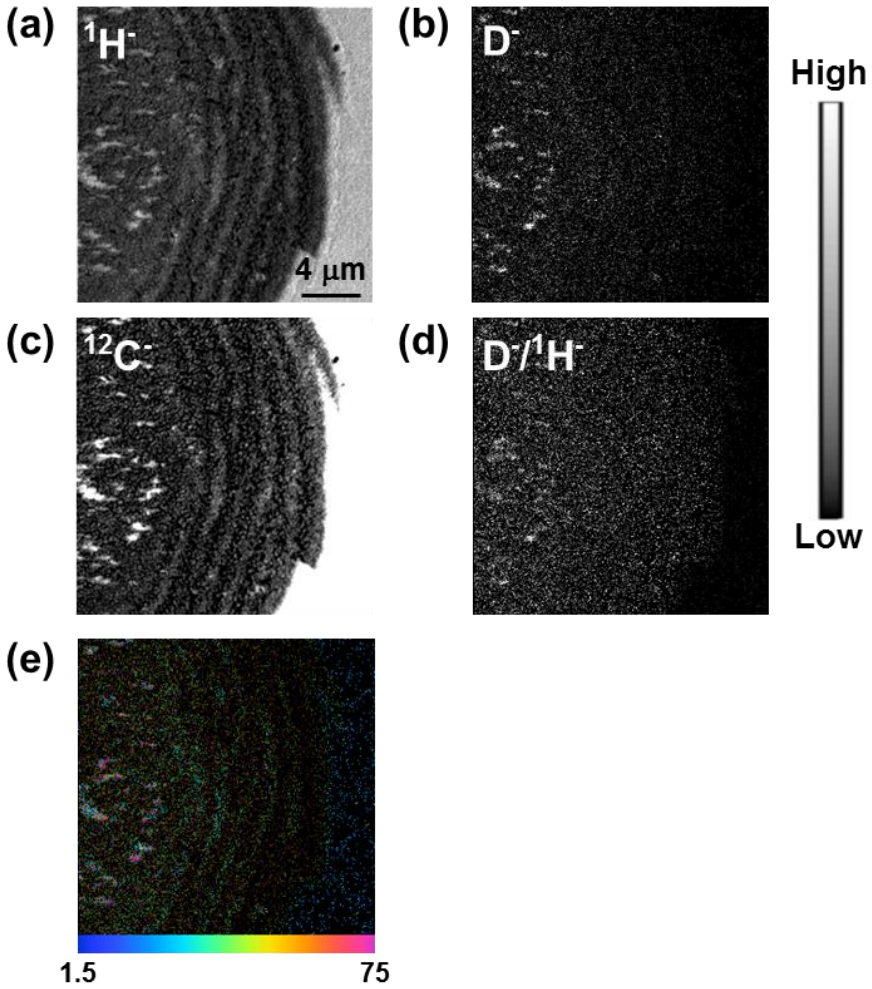

Figure 6.5 NanoSIMS images of cross-section of the hair dyed with pPD-d4 and pAOC: (a) $^1H^-$ image, (b) D^- image, (c) $^{12}C^-$ image, (d) $D^-/^1H^-$ ratio image, and (e) HSI $D^-/^1H^-$ ratio image; the color scale represents the value of the ratio × 10,000. The scale ranges from blue (natural abundance ratio of deuterium, 0.015%) to red (0.75%, 50 times the natural ratio) [Lechene et al., 2006; McMahon et al., 2006].

6.4. Summary

The thickness of hair cuticle layers could be widened by improving the method used for preparing of hair cross-section.

NanoSIMS analysis using the improved hair cross-section preparation method revealed that more colored chromophores formed by oxidative dyeing were fixated in the endocuticle than in the other fine structures of the cuticle layer, and the dyeing behavior of oxidative dyes in fine structures of the hair cuticle was substantiated.

Chapter 7
Summary and Conclusions

In this thesis, to better understand the functional mechanisms of hair cosmetics on human hair, two types of SIMS, TOF-SIMS and NanoSIMS, were used, and the advantages of each analysis technique were exploited.

In Chapter 2, the penetration and adsorption of two cosmetic ingredients, L-theanine and cationic chitosan, on hair were investigated by TOF-SIMS. By using deuterium-labeled L-theanine, the deuterium ion at *m/z* 2 could be used as a characteristic fragment ion peak of L-theanine. The deuterium ion peak was clearly detected from the negative TOF-SIMS spectrum of the damaged hair treated using deuterium-labeled L-theanine. A deuterium ion mapping image of TOF-SIMS revealed that L-theanine penetrated deeply and was distributed uniformly over the damaged hair inside.

To investigate the adsorption of cationic chitosan on the hair surface, a more suitable fragment ion peak was selected from the positive TOF-SIMS spectra of cationic chitosan. In the TOF-SIMS spectra of hairs treated using cationic chitosan, the peak at *m/z* 102 was more clearly detected from bleached hair than from virgin hair. The mapping image of the *m/z* 102 ion of TOF-SIMS indicated that cationic chitosan was uniformly adsorbed on the hair surface and that the amount of cationic chitosan adsorbed on bleached hair was more than that on virgin hair.

In Chapter 3, the conditioning effect of a vegetable oil, hydrogenated palm oil, for damaged hair was evaluated, and the permeability of hydrogenated palm oil was investigated by TOF-SIMS. It was indicated that a conditioner containing hydrogenated palm oil had greater inhibitory effect on water swelling than a control conditioner. Tripalmitin, which was used as an indicator of hydrogenated palm oil, was clearly detected from an extract of hair treated with a conditioner containing it. Deuterium-labeled tripalmitin was used to improve the sensitivity of TOF-SIMS analysis. A deuterium ion peak was clearly observed in the negative TOF-SIMS

spectrum of the cross-section of damaged hair treated with a conditioner containing deuterium-labeled tripalmitin. A deuterium ion mapping image of TOF-SIMS confirmed that deuterium-labeled tripalmitin penetrated damaged hair and localized around the perimeter. TOF-SIMS ion mapping images combined with an LSM image revealed that tripalmitin penetrated the cuticle and outer cortex of damaged hair. The TOF-SIMS analysis results suggested that hydrogenated palm oil's great inhibitory effect on water swelling was due to its penetration of the cuticle and outer cortex of damaged hair.

In Chapter 4, the influence of bleach treatment on the chemical composition of human hair melanin was investigated by NanoSIMS. In a NanoSIMS $^{16}O^-$ ion image of hair cross-sections, $^{16}O^-$ ions were intensely detected from several hundred nanometer-sized particulate regions in the cortex of both virgin black hair and bleached hair. From the NanoSIMS $^{16}O^-$ ion image and the LSM images of the hair cross-sections, the particulate regions, where $^{16}O^-$ ions were intensely detected in the NanoSIMS image, were identified as melanin granules. More intensive $^{16}O^-$ ions were detected from the melanin granules of bleached hair than from those of virgin black hair. The ion intensity values of particulate regions, where $^{16}O^-$ ions were intensely detected in the NanoSIMS image of hair cross-sections, were calculated, and data analysis was performed using these values. It was indicated that the $^{16}O^-$ ion intensity and $^{16}O^-/^{12}C^{14}N^-$ ion intensity ratio of melanin granules in bleached hair were higher than those in virgin black hair. The NanoSIMS analysis of the cross-sections of virgin black hair and bleached hair indicated that bleach treatment increased the oxygen content in melanin granules.

In Chapter 5, the dyeing regions of oxidative hair dyes in the fine structure of human hair were investigated by using a stable isotope-labeled oxidative dye with NanoSIMS. The visible spectra of methanol extracts obtained from dyed hairs indicated that pPD-d4 reacts with pAOC in a manner very similar to pPD. In a positive TOF-SIMS spectrum of an extract obtained from hair dyed with pPD-d4 and pAOC, an ion peak at *m/z* 232, corresponding to deuterium-labeled binuclear indo dye formed from pPD-d4 and pAOC, was detected, and it was indicated that the deuterium ion can

be used as a characteristic fragment ion for the colored chromophore formed from pPD-d4 and pAOC. NanoSIMS images of cross-sections of hair dyed with pPD-d4 and pAOC indicated that colored chromophores were frequently formed in nano-sized particulate constituents of black hair. From a comparison of the dyeing behaviors of black and white hair, particulate regions in which deuterium ions were intensely detected in the dyed black hair were identified as melanin granules. NanoSIMS analysis revealed that melanin granules are one of the most important dyeing regions for oxidative hair coloring.

In Chapter 6, the dyeing behavior in fine structures of the hair cuticle was especially focused on, and the dyeing regions of oxidative hair dyes were investigated by using a stable isotope-labeled oxidative dye with NanoSIMS. To widen the thickness of cuticle layers, hair was embedded diagonally to the cutting surface in resin and cross-sectioned. As a result, an elliptical, laterally widened hair cross-section was obtained, and the thickness of a cuticle layer in the hair cross-section was increased by approximately three times. By comparing the AFM image and NanoSIMS $^{12}C^-$ image of hair cross-sections made by the improved preparation method, it was confirmed that $^{12}C^-$ ions were strongly detected from the cystine-poor region (endocuticle) in comparison with the cystine-rich regions (A-layer and exocuticle). HSI transformation of the NanoSIMS $D^-/^1H^-$ ratio image was performed to increase the contrast of the isotope ratio data. As a result, it was confirmed that the regions corresponding to the endocuticle had a higher $D^-/^1H^-$ ratio than other fine structures of the cuticle layer. The NanoSIMS images of the dyed hair substantiated that more colored chromophores formed by oxidative dyeing were fixated in the endocuticle than in the other fine structures of the cuticle layer.

In this thesis, two types of SIMS having different characteristic were used. The permeability behaviors of conditioning agents inside the hair could be revealed by TOF-SIMS analyses using deuterium-labeled compounds of interest. Further, the adsorptive behaviors of a cationic polymer on the hair surface could be investigated by selecting a more suitable fragment ion peak of the cationic polymer in the TOF-SIMS spectrum instead of the most intensive fragment ion peak. The compositional changes of

melanin granules resulting from bleach treatment could be directly observed by NanoSIMS without isolating melanin. Additionally, the behaviors of the active ingredients of oxidative hair colorant, oxidative dyes, on the micro regions of hair could be revealed by a combination of the NanoSIMS and isotope labeling techniques. This thesis indicates that SIMS is one of the most powerful analytical techniques for investigating the effects of hair cosmetics on human hair and that it provides valuable information for cosmetic chemists. The effective use of SIMS for hair research will lead to a better understanding of the functional mechanisms of hair cosmetics in the future.

By advancing the development of hair cosmetics on the basis of the new knowledge obtained from understanding of the functional mechanisms, the performances of current hair cosmetics will be improved. Hair cosmetics, which have high performance and high satisfaction, help realize healthy and beautiful head hair, and they will play a role in improving the quality of people’s lives.

References

Arnaud JC, Bore P (**1981)** Isolation of melanin pigments from human hair. J. Soc. Cosmet. Chem. 32: 137−152.

Audinot J-N, Schneider S, Yegles M, Hallegot P, Wennig R, Migeon H-N (**2004**) Imaging of arsenic traces in human hair by nano-SIMS 50. Appl. Surf. Sci. 231−232: 490−496.

Bantignies J-L, Fuchs G, Carr GL, Williams GP, Lutz D, Marull S (**1998**) Organic reagent interaction with hair spatially characterized by infrared microspectroscopy using synchrotron radiation. Int. J. Cosmet. Sci. 20: 381−394.

Bantignies J-L, Carr GL, Lutz D, Marull S, Williams GP, Fuchs G (**2000**) Chemical imaging of hair by infrared microspectroscopy using synchrotron radiation. J. Cosmet. Sci. 51: 73−90.

Beard BC, Johnson A, Cambria FM, Trinh PN (**2005**) Electron spectroscopy and microscopy applied chemical and structural analysis of hair. J. Cosmet. Sci. 56: 65−77.

Berthiaume MD, Merrifield JH, Riccio DA (**1995**) Effects of silicone pretreatment on oxidative hair damage. J. Soc. Cosmet. Chem. 46: 231−245.

Bhushan B (**2010**) Introduction-human hair, skin, and hair care products. In: Biophysics of human hair. Springer-Verlag, Berlin, Chapter 1, pp. 1−19.

Borges CR, Roberts JC, Wilkins DG, Rollins DE (**2001**) Relationship of melanin degradation products to actual melanin content: application to human hair. Anal. Biochem. 290: 116−125.

Boxer SG, Kraft ML, Weber PK (**2009**) Advances in imaging secondary ion mass spectrometry for biological samples. Annu. Rev. Biophys. 38: 53−74.

Brown KC (**1997**) Hair coloring. In: Johnson DH (ed) Hair and hair care. Marcel Dekker, Inc., New York, Chapter 7, pp. 191−215.

Chao J, Newsom AE, Wainwright IM, Mathews RA (**1979**) Comparison of the effects of some reactive chemicals on the proteins of whole hair, cuticle and cortex. J. Soc. Cosmet. Chem. 30: 401−413.

Chen N, Bhushan B (**2005**) Morphological, nanomechanical and cellular structural characterization of human hair and conditioner distribution using torsional resonance mode with an atomic force microscope. J. Microsc. 220: 96−112.

Clode PL, Stern RA, Marshall AT (**2007**) Subcellular imaging of isotopically labeled carbon compounds in a biological sample by ion microprobe (NanoSIMS). Microsc. Res. Tech. 70: 220−229.

Clode PL, Kilburn MR, Jones DL, Stockdale EA, Cliff III JB, Herrmann AM, Murphy DV (**2009**) In situ mapping of nutrient uptake in the rhizosphere using nanoscale secondary ion mass spectrometry. Plant Physiol. 151: 1751−1757.

Corbett JF (**1973**) The role of meta difunctional benzene derivatives in oxidative hair dyeing. I. Reaction with p-diamines. J. Soc. Cosmet. Chem. 24: 103−134.

Corcuff P, Gremillet P, Jourlin M, Duvault Y, Leroy F, Leveque JL (**1993**) 3D Reconstruction of human hair by confocal microscopy. J. Soc. Cosmet. Chem. 44: 1−12.

Formanek F, De Wilde Y, Luengo GS, Querleux B (**2006**) Investigation of dyed human hair fibers using apertureless near-field scanning optical microscopy. J. Microsc. 224: 197−202.

Gruber JV, Winnik FM, Lapierre A, Khaloo ND, Joshi N, Konish PN (**2001**) Examining cationic polysaccharide deposition onto keratin surfaces through biopolymer fluorescent labeling. J. Cosmet. Sci. 52: 119−129.

Gummer GL (**2001**) Elucidating penetration pathways into the hair fiber using novel microscopic techniques. J. Cosmet. Sci. 52: 265−280.

Gumprecht JG, Patel K, Bono RP (**1977**) Effective of reduction and oxidation in acid and alkaline permanent waving. J. Soc. Cosmet. Chem. 28: 717−732.

Habe T, Tanji N, Inoue S, Okamoto M, Tokunaga S, Tanamachi H (**2011**) TOF-SIMS characterization of the lipid layer on the hair surface. I: the damage caused by chemical treatments and UV radiation. Surf. Interface Anal. 43: 410−412.

Hallegot P, Corcuff P (**1993**) High-spatial-resolution maps of sulphur from human hair sections; an EELS study. J. Microsc. 172: 131−136.

Hallegot P, Peteranderl R, Lechene C (**2004**) In-situ imaging mass spectrometry analysis of melanin granules in the human hair shaft. J. Invest. Dermatol. 122: 381−386.

Harvey A, Carr CM, Pereira A (**2004**) Time-of-flight secondary ion mass spectrometry (ToF-SIMS) analysis of the application of a cationic conditioner to “clean” hair. J. Cosmet. Sci. 55: 265−279.

Herrmann AM, Ritz K, Nunan N, Clode PL, Pett-Ridge J, Kilburn MR, Murphy DV, O’Donnell AG, Stockdale EA (**2007**) Nano-scale secondary ion mass spectrometry – A new analytical tool in biogeochemistry and soil ecology: A review article. Soil. Biol. Biochem. 39: 1835−1850.

Hoshowski MA (**1997**) Conditioning of hair. In: Johnson DH (ed) Hair and hair care. Marcel Dekker, Inc., New York, Chapter 4, pp. 65−104.

Imai T, Niwa M, Hasegawa T, Kawamura H, Umemura T, Kimura M, Nakano T, Haraguchi H (**2008**) The reaction of oxidative hair dyes in cuticle layers (in Japanese). J. Soc. Cosmet. Chem. Jpn. 42: 305−312.

Imai T, Niwa M, Kawamura H, Umemura T, Kimura M, Nakano T (**2010**) The dyeing mechanism of oxidative hair color in white and black human hair (in Japanese). J. Soc. Cosmet .Chem. Jpn. 44: 208−215.

Imai T (**2011**) The influence of hair bleach on the ultrastructure of human hair with special reference to hair damage. Okajimas Folia Anat. Jpn. 88: 1−9.

Ito S, Wakamatsu K, Ozeki H (**2000**) Chemical analysis of melanins and its application to the study of the regulation of melanogenesis. Pigment Cell Res. 13: 103−109.

Ito S, Wakamatsu K (**2008**) Chemistry of mixed melanogenesis—pivotal roles of dopaquinone. Photochem. Photobiol. 84: 582−592.

Ito S, Nakanishi Y, Valenzuela RK, Brilliant MH, Kolbe L, Wakamatsu K (**2011**) Usefulness of alkaline hydrogen peroxide oxidation to analyze eumelanin and pheomelanin in various tissue samples: application to chemical analysis of human hair melanins. Pigment Cell Melanoma Res. 24: 605−613.

Jachowicz J (**1987**) Hair damage and attempts to its repair. J. Soc. Cosmet. Chem. 38: 263−286.

Jones LN, Rivett DE (**1997**) The role of 18-methyleicosanoic acid the structure and formation of mammalian hair fibers, Micron. 28: 469−485.

Kassenbeck P (**1981**) Morphology and fine structure of hair. In: Orfanos C, Montagna W, Stuttgen G (eds) Hair Research, Springer-Verlag, Berlin, pp. 52−64.

Keis K, Persaud D, Kamath YK, Rele AS (**2005**) Investigation of penetration abilities of various oils into human hair fibers. J. Cosmet. Sci. 56: 283−295.

Keis K, Huemmer CL, Kamath YK (**2007**) Effect of oil films on moisture vapor adsorption on human hair. J. Cosmet. Sci. 58: 135−145.

Kelch A, Wessel S, Will T, Hintze U, Wepe R, Wiesendanger R (**2000**) Penetration pathway of fluorescent dyes in human hair fibers investigated by scanning near-field optical microscopy. J. Microsc. 200: 179−186.

Kempson IM, Skinner WM (**2005**) ToF-SIMS analysis of elemental distributions in human hair. Sci. Total Environ. 338: 213−227.

Kitano H (**2008**) Study of fine-structures and mechanical properties of human hair by using atomic force microscopy (in Japanese). Hyomen Kagaku 29: 427−431.

Kitano H, Yamamoto A, Yamanouchi S, Kojima T, Niwa M, Fujinami S, Nakajima K, Nishi T, Naito S (**2008**) Effects of chemical treatments on mechanical properties of hair internal components by atomic force microscopy. In Proceeding of 25th International Federation of Societies of Cosmetic Chemists (IFSCC) Congress. Barcelona, Spain.

Kitano H, Yamamoto A, Niwa M, Fujinami S, Nakajima K, Nishi T, Naito S (**2009**) Young's modulus mapping on hair cross-section by atomic force microscopy. Compos. Interfaces 16: 1−9.

Klemm EJ, Haefele JW, Thomas AR (**1965**) The swelling behavior of hair fibers in lithium bromide. Proc. Sci. Sect. Toilet Goods Assoc. 43: 7−13

Korytowski W, Sarna T (**1990**) Bleaching of melanin pigments. J. Biol. Chem. 265: 12410−12416.

Kuzuhara A, Hori T (**2003**) Reduction mechanism of tioglycolic acid on keratin fibers using microspectrophotometry and FT-Raman spectrometry. Polymer 44: 7963−7970.

Kuzuhara A (**2005**) Analysis of structural change in keratin fibers resulting from chemical treatments using Raman spectroscopy. Biopolymers 77: 335−344.

Kuzuhara A (**2006**) Analysis of structural changes in bleached keratin fibers (black and white human hair) using Raman spectroscopy. Biopolymers 81: 506−514.

Kuzuhara A (**2007**) Analysis of structural changes in permanent waved human hair using Raman spectroscopy. Biopolymers 85: 274−283.

Kuzuhara A (**2011**) Raman spectroscopic analysis of L-phenylalanine and hydrolyzed eggwhite protein penetration into keratin fibers. J. Appl. Polym. Sci. 122: 2680−2689.

Kuzuhara A (**2013**) Analysis of internal structure changes in black human hair keratin fibers resulting from bleaching treatments using Raman spectroscopy. J. Mol. Struct. 1047: 186−193.

Lechene C, Hillion F, McMahon G, Benson D, Kleinfeld AM, Kampf JP, Distel D, Luyten Y, Bonventre J, Hentschel D, Park KM, Ito S, Schwartz M, Benichou G, Slodzian G (**2006**) High-resolution quantitative imaging of mammalian and bacterial cells using stable isotope mass spectrometry. J. Biol. 5: 20.

Liu Y, Kempf VR, Nofsinger JB, Weinert EE, Rudnicki M, Wakamatsu K, Ito S, Simon JD (**2003**) Comparison of the structural and physical properties of human hair eumelanin following enzymatic or acid/base extraction. Pigment Cell Res. 16: 355−365.

Lochhead RY (**2012**) Shampoo and Conditioner science. In: Evans T, Wickett RR (eds) Practical modern hair science. Allured Business Media, Illinois, Chapter 3, pp. 75−116.

Marsh JM (**2012**) Hair coloring. In: Evans T, Wickett RR (eds) Practical modern hair science. Allured Business Media, Illinois, Chapter 4, pp. 117−155.

Masukawa Y, Tsujimura H, Tanamachi H, Narita H, Imokawa G (**2004**) Damage to human hair caused by repeated bleaching combined with daily weathering during daily life activities. Exog. Dermatol. 3: 273−281.

Masukawa Y, Shimogaki H, Manago K, Imokawa G (**2005**) A novel method for visualizing hair lipids at the cell membrane complex: Argon sputter etching/scanning electron microscopy. J. Cosmet. Sci. 56: 297−309.

Masukawa Y, Tanamachi H, Tsujimura H, Mamada A, Imokawa G (**2006**) Characterization of hair lipid images by argon sputter etching–scanning electron microscopy. Lipids 41: 197−205.

Matsushita Y, Sekiguchi T, Saito K, Kato T, Imai T, Fukushima K (**2007**) The characteristic fragment ions and visualization of cationic starches on pulp fiber using TOF-SIMS. Surf. Interface Anal. 39: 501−505.

McMahon G, Glassner BJ, Lechene CP (**2006**) Quantitative imaging of cells with multi-isotope imaging mass spectrometry (MIMS)—Nanoautography with stable isotope tracers. Appl. Surf. Sci. 252: 6895−6906.

Menkart J, Wolfram LJ, Mao I (**1966**) Caucasian hair, Negro hair, and wool: similarities and differences. J. Soc. Cosmet. Chem. 17: 769−787.

Menon IA, Persad S, Haberman HF, Kurian CJ (**1983**) A comparative study of the physical and chemical properties of melanins isolated from human black and red hair. J. Invest. Dermatol. 122: 202−206.

Morel OJX, Chrestie RM (**2011**) Current trends in the chemistry of permanent hair dyeing. Chem. Rev. 111: 2537-2561.

Naito S, Oshima K (**1987**) The adsorption of keratin hydrolysate to hair and its effect (in Japanese). J. Soc. Cosmet. Chem. Jpn. 21: 146−155.

Naito S, Takahashi T, Hattori M, Arai K (**1992**) Histochemical observation of the cell membrane complex of hair. SENIGAKKAISHI 48: 420−426.

Negri AP, Cornell HJ, Rivett DE (**1993**) A model for the surface of keratin fibers. Textile Res. J. 63: 109−115.

Nishida Y, Ito T, Hosokawa M, Aono M, Yokomaku A, Konta H, Iimura K, Kato T, Sugiyama K (**2004**) Repairing effects of diglucosyl gallic acid on coloring-damaged hair. J. Oleo Sci. 53: 295−304.

Okamoto M, Tanji N, Habe T, Inoue S, Tokunaga S, Tanamachi H (**2011**) TOF-SIMS characterization of the lipid layer on the hair surface. II: effect of the 18-MEA lipid layer on surface hydrophobicity. Surf. Interface Anal. 43: 298−301.

Pillai ZS, Kamat PV (**2005**) Spectroelectrochemistry of aromatic amine oxidation: an insight into the indo dye formation. Res. Chem. Intermed. 31: 103−112.

Popescu C, Höcker H (**2007**) Hair-the most sophisticated biological composite material. Chem. Soc. Rev. 36: 1282−1291.

Popescu C (**2012**) Hair damage. In: Evans T, Wickett RR (eds) Practical modern hair science. Allured Business Media, Illinois, Chapter 11, pp. 367−388.

Prota G (**1988**) Progress in the chemistry of melanins and related metabolites. Med. Res. Rev. 8: 525−556.

Prota G (**1997**) Pigment cell research: What directions? Pigment Cell Res. 10: 5−11.

Regismond STA, Heng Y-M, Goddard ED, Winnik FM (**1999**) Fluorescence microscopy observation of the adsorption onto hair of a fluorescently labeled cationic cellulose ether. Langmuir 15: 3007−3010.

Rele AS, Mohile RB (**2003**) Effect of mineral oil, sunflower oil, and coconut oil on prevention hair damage. J. Cosmet. Sci. 54: 175−192.

Riley PA (**1997**) Melanin. Int. J. Biochem. Cell Biol. 29: 1235−1239.

Robbins CR, Kelly C (**1969**) Amino acid analysis of cosmetically altered hair. J. Soc. Cosmet. Chem. 20: 555−564.

Robbins CR, Bahl MK (**1984**) Analysis of hair by electron spectroscopy for chemical analysis. J. Soc. Cosmet. Chem. 35: 379−390.

Robbins CR (**2012a**) Morphological, macromolecular structure and hair growth. In: Chemical and physical behavior of human hair, 5th edition. Springer-Verlag, Berlin, Chapter 1, pp. 1−104.

Robbins CR (**2012b**) Reducing human hair including permanent waving and straighting. In: Chemical and physical behavior of human hair, 5th edition. Springer-Verlag, Berlin, Chapter 4, pp. 205−262.

Robbins CR (**2012c**) Bleaching and oxidation of human hair. In: Chemical and physical behavior of human hair, 5th edition. Springer-Verlag, Berlin, Chapter 5, pp. 263−328.

Robbins CR (**2012d**) Dyeing human hair. In: Chemical and physical behavior of human hair, 5th edition. Springer-Verlag, Berlin, Chapter 7, pp. 444−488.

Ruetsch SB, Kamath YK, Rele AS, Mohile RB (**2001**) Secondary ion mass spectrometric investigation of penetration of coconut and mineral oils into human hair fibers: Relevance to hair damage. J. Cosmet. Sci. 52: 162−184.

Ruetsch SB, Kamath YK (**2005**) Penetration of cationic conditioning compounds into hair fibers: A TOF-SIMS approach. J. Cosmet. Sci. 56: 323−330.

Saito K, Mitsutani T, Imai T, Matsushita Y, Fukushima K (**2008**) Discriminating the indistinguishable sapwood from heartwood in discolored ancient wood by direct molecular mapping of specific extractives using time-of-flight secondary ion mass spectrometry. Anal. Chem. 80: 1552−1557.

Saito K, Watanabe Y, Shirakawa M, Matsushita Y, Imai T, Koike T, Sano Y, Funada R, Fukuzawa K, Fukushima K (**2012**) Direct mapping of morphological distribution of syringyl and guaiacyl lignin in the xylem of maple by time-of-flight secondary ion mass spectrometry. The Plant J. 69: 542−552.

Sakamoto O, Fujinuma Y, Ozawa T, Katsura H (**1978**) A study on isolation and solubilization of human hair melanin and its application for the colorimetric determination of melanin in the hair bleached in various degrees (in Japanese). J. Soc. Cosmet. Chem. Jpn. 12: 39−45.

Slawinska D, Slawinski J (**1982**) Electronically excited molecules in the formation and degradation of melanins. J. Physiol. Chem. Phys. 14: 363−374.

Smart KE, Kilburn M, Schroeder M, Martin BGH, Hawes C, Marsh JM, Gronvenor CRM (**2009**) Copper and calcium uptake in colored hair. J. Cosmet. Soc. 60: 337−386.

Staudigel JA, Bunasky K, Gamsky CJ, Wagner MS, Stump KJ, Baker JM, Mapple RM, Thomas JH (**2007**) Use of quaternized cassia galactomannan for hair conditioning, J. Cosmet. Sci. 58: 637−650.

Strassburger J, Breuer MM (**1985**) Quantitative Fourier transform infrared spectroscopy of oxidized hair, J. Soc. Cosmet. Chem. 36: 61−74.

Swift JA (**1992**) Swelling of human hair by water. Proceedings of the 8th international hair science symposium of the DWI, Kiel, Germany, 9−11 Sept.

Swift JA (**1997**) Morphology and histochemistry of human hair. In: Jollès H, Zahn H, Höcher H (eds) Formation and structure of human hair. Birkhauser Verlag, Basel, pp. 149−175.

Swift JA (**1999**) Human hair cuticle: Biologically conspired to owner's advantage. J. Cosmet. Sci. 50: 23−47.

Swift JA, Chahal SP, Challoner NI, Parfrey JE (**2000**) Investigations on the penetration of hydrolyzed wheat proteins into human hair by confocal laser-scanning fluorescence microscopy. J. Cosmet. Sci. 51: 193−203.

Takada K, Nakamura A, Matsuo N, Inoue A, Someya K, Shimogaki H (**2003**) Influence of oxidative and/or reductive treatment on human hair (I): analysis of hair-damage after oxidative and/or reductive treatment. J. Oleo Sci. 10: 541−548.

Tanamachi H, Okamoto Y, Fujiwara N, Tsujimura H, Sonoda J, Naito S, Sugai Y (**2004**) Prevention effects of lipid-related materials on human hair damage progress. J. Cosmet. Sci. 55: S171−S173.

Tate ML, Kamath YK, Ruetsch SB, Weigmann H-D (**1993**) Quantification and prevention of hair damage. J. Soc. Cosmet. Chem. 44: 347−371.

Watanabe S, Kanetaka S, Miyata K, Nakamura Y (**1994**) A consideration on the distribution of metal elements in human hair (in Japanese). J. Soc. Cosmet. Chem. Jpn. 28: 262−269.

Wickett RR (**2012)** Changing the shape of hair. In: Evans T, Wickett RR (eds) Practical modern hair science. Allured Business Media, Illinois, Chapter 5, pp. 157−192.

Williams P (**2006**) Biological imaging using secondary ions. J. Biol. 5: 18.

Wilmsmann H (**1961**) Beziehungen Zwischen Der Molekülgrösse Aromatischer Verbindungen Und Ihrem Penetrationsvermögen Für Das Menschliche Haar. J. Soc. Cosmet. Chem. 12: 490−500.

Wolfram LJ, Hall K, Hui I (**1970**) The mechanism of hair bleaching. J. Soc. Cosmet. Chem. 21: 875−900.

Wortmann F-J, Kure N (**1985**) Torsional behavior of human hair. J. Soc. Cosmet. Chem. 36: 87−99.

Wortmann F-J, Kure N (**1990**) Bending relaxation properties of human hair and permanent waving performance. J. Soc. Cosmet. Chem. 41: 123−139.

Wortmann F-J, Wortmann G, Zahn H (**1997**) Pathways for dye diffusion in wool fibers. Textile Res. J. 67, 720−724.

Zvaik C, Dawber RPR (**1986**) Hair structure, function and physicochemical properties. In: Zvaik C (ed) The science of hair care. Marcel Dekker, Inc New York, Chapter 1, pp. 1−48.

Zvaik C (**1986**) Oxidation coloring. In: Zvaik C (ed) The science of hair care. Marcel Dekker, Inc., New York, Chapter 8, pp. 263−286.

Acknowledgements

The works in this thesis were carried out during the period from 2007 to 2014 under the guidance of Professor Kazuhiko Fukushima in the Laboratory of Forest Chemistry, Graduate School of Bioagricultural Sciences, Nagoya University, and in the Fundamental Research Laboratory, General Research & Development Institute, Hoyu. Co., Ltd.

The author would like to express sincere gratitude to Professor Kazuhiko Fukushima for his excellent guidance, invaluable suggestions, and assistance throughout this study.

The author is very grateful to Associate Professor Yasuyuki Matsushita and Assistant Professor Dan Aoki, Laboratory of Forest Chemistry, Graduate School of Bioagricultural Sciences, Nagoya University, for their helpful advice and valuable suggestions.

The author is also grateful to Dr. Kaori Saito for her kind support in the TOF-SIMS studies.

The author is grateful to Project Research Associate Miyuki Takeuchi, Department of Biomaterial Sciences, Graduate School of Agricultural and Life Sciences, The University of Tokyo, for her support in performing the NanoSIMS measurements and discussions about the NanoSIMS data.

The author thanks Toshiyuki Kato and Ruka Takama, Technical Center, Nagoya University, for their support in performing the TOF-SIMS measurements and the ESI-TOF-MS measurements.

The author wishes to express his gratitude to Dr. Masanao Niwa and Toshihiko Yamamoto in the General Research & Development Institute, Hoyu Co., Ltd., for providing him with the opportunity of this work.

The author also wishes to thank his superiors and colleagues, Mitsuru Isobe, Masakatu Hata, Dr. Hiroki Kitano, Dr. Teppei Nawa, Tsuji Shiho, Hiromi Yamada, and Yukari Saito, in the General Research & Development Institute, Hoyu Co., Ltd., for their kind cooperation.

Finally, the author would like to thank his wife Sayuri, daughter Hinano, and son Kakeru for their warm support and encouragement.

Toru Kojima

List of publications concerning the thesis

Original papers

1) **Toru Kojima**, Hiroki Kitano, Masanao Niwa, Kaori Saito, Yasuyuki Matsushita, and Kazuhiko Fukushima
Imaging analysis of cosmetic ingredients interacted with human hair using TOF-SIMS
Surface and Interface Analysis **2011**, 43, 562−565. **(Chapter 2)**

2) **Toru Kojima**, Shiho Tsuji, Masanao Niwa, Kaori Saito, Yasuyuki Matsushita, and Kazuhiko Fukushima
Distribution analysis of triglyceride having repair effect on damaged human hair by TOF-SIMS
International Journal of Polymer Analysis and Characterization **2012**, 17, 21−28. **(Chapter 3)**

3) **Toru Kojima**, Hiromi Yamada, Toshihiko Yamamoto, Yasuyuki Matsushita, and Kazuhiko Fukushima
Dyeing regions of oxidative hair dyes in human hair investigated by nanoscale secondary ion mass spectrometry
Colloids and Surfaces B: Biointerfaces **2013**, 106, 140−144. **(Chapter 5)**

4) **Toru Kojima**, Hiromi Yamada, Mitsuru Isobe, Toshihiko Yamamoto, Miyuki Takeuchi, Dan Aoki, Yasuyuki Matsushita, and Kazuhiko Fukushima
Compositional changes of human hair melanin resulting from bleach treatment investigated by nanoscale secondary ion mass spectrometry
Skin Research and Technology **2014**, 20, 416−421. **(Chapter 4)**

5) **Toru Kojima**, Hiromi Yamada, Yukari Saito, Teppei Nawa, Mitsuru Isobe, Toshihiko Yamamoto, Dan Aoki, Yasuyuki Matsushita, and Kazuhiko Fukushima
Investigation of dyeing behavior of oxidative dye in fine structures of the human hair cuticle by nanoscale secondary ion mass spectrometry
Skin Research and Technology **2014** (DOI: 10.1111/srt.12192) **(Chapter 6)**

Reference

1) 小島徹
「二次イオン質量分析法を用いた酸化染料の毛髪内染着部位に関する研究」
FRAGRANCE JOURNAL 2014 年 3 月号(Vol.42, No.3)通巻 405, 12-16.